

Reflection and Transmission of Radio Waves at a Continuously Stratified Plasma With Arbitrary Magnetic Induction^{1, 2}

J. Ralph Johler and John D. Harper, Jr.

Contribution From Central Radio Propagation Laboratory, National Bureau of Standards, Boulder, Colo.

(Received July 6, 1961; revised July 21, 1961)

A flexible theoretical model plasma which can be deformed to fit most measured electron-ion-altitude profiles is employed together with available geophysical data on the ionosphere to evaluate reflections and transmissions during quiescent and disturbed propagation conditions. The reflections and transmissions in the ionosphere are determined rigorously with the aid of the classical magneto-ionic theory. The complex indexes of refraction of the medium are deduced, and a coupling in the plasma between ordinary and extraordinary, upgoing and downgoing modes of propagation is investigated. The corresponding reflection and transmission coefficients are then calculated, and certain phenomena which can be expected as a result of the action of a solar disturbance on the reflection process are predicted.

The disturbance of solar origin, investigated as an application of developed techniques, influences the reflected and transmitted LF waves in the lower ionosphere in a complicated manner. However, the high absorption phenomena exhibited by high frequencies do not seem to exist for the plasma profiles investigated with the classical magneto-ionic theory.

The electron-collision frequencies of the classical magneto-ionic theory are modified to introduce a collision frequency proportional to the electron energy, and the changes necessary in the formulation of the classical theory as a result of such a consideration are presented.

1. Introduction

Low-frequency radio navigation and communication systems utilize or are capable of utilizing ionospheric modes of propagation, especially those systems with great distance transmissions. Indeed, the nature of low-radiofrequency wave propagation around the earth is, in large measure, determined by the shape of the lower ionosphere electron-ion density transitional region, i.e., the lower 40–100 km electron density-altitude, $N(h)$, collision frequency-altitude, $\nu(h)$, profiles of the ionosphere. Previous theoretical treatment of the reflection process [Johler and Walters, 1960] at low radiofrequencies uses a sharply bounded model electron-ion plasma.

Experimental evidence [Johler, 1961] indicates that such a profile is not always a valid model. Thus, especially in the case of an ionosphere disturbance, it seems to be appropriate to utilize a theory which takes into consideration in more detail the changes within the ionosphere which affect the reflection process. This paper extends the theory previously presented [Johler and Walters, 1960] to a flexible theoretical model which can be mutilated to fit rigorously almost any measured $N(h)$, $\nu(h)$ profiles. The theory can therefore treat physical changes within the ionosphere as such changes affect the reflection and transmission processes and, in particular, the theory can treat a plasma reflection and transmission region with electron-ion density transitions of quite arbitrary form.

The newly developed model and associated techniques of analysis are then applied to certain geophysical and theoretical data in the form of the $N(h)$, $\nu(h)$ profiles of the lower ionosphere during both quiescent and disturbed propagation conditions. The effect, if any, of a solar disturbance upon communication circuits which utilize low-frequency propagation is ascertained.

¹ This is an extended and revised version of a paper presented at a special meeting on disturbances of solar origin, of the Avionics Panel of the Advisory Group for Aeronautical Research and Development (AGARD), NATO, Naples, Italy, May 1961.

² This work was sponsored by the United States Air Force, Rome Air Development Center, Griffiss Air Force Base, N. Y., and performed in connection with tasks 4 and 5 of delivery order A F 30(602)-2488 dated March 29, 1961.

The classical magneto-ionic theory is modified by the introduction of the concept of an electron-collision frequency proportional to the electron thermal energy [Jancel and Kahan, 1955; Dingle, Arndt, and Roy, 1959; Molmud, 1959; and Phelps, 1960] into the analysis of the reflection and transmission process at the plasma with transitional electron-ion density.

2. Determination of the Indexes of Refraction of the Medium

The lower boundary of the model electron-ion plasma, figure 1, below which ($z < 0$) the ionization is nil ($N=0$), is considered to be the xy -plane. The region above the xy -plane ($z > 0$) is characterized by an electron density, N , and a collision frequency, ν , which vary arbitrarily with respect to altitude, z . A plane wave, \bar{E}_i ,

$$E_i = |\bar{E}_i| \exp \left[i \left(\omega t - \frac{\omega}{c} \eta D \right) \right], \quad (1)$$

is incident upon the plasma from the lower region ($z < 0$), where the index of refraction ($z < 0$), $\eta = \eta_0 = 1$, and c is the speed of light, $c \sim 3 \times 10^8$ meters/second. The quantity D can be defined with respect to quantities in figure 1,

$$D = x \sin \phi_i \sin \phi_a + y \sin \phi_i \cos \phi_a + z \cos \phi_i. \quad (2)$$

The field, \bar{E}_i , is varying harmonically in time, t , at a frequency $f = \omega/2\pi$. The field also is assumed to be incident upon the xy -plane at an angle of incidence, ϕ_i , and a direction of propagation or magnetic azimuth, ϕ_a , measured clockwise from the yz -plane, figure 1. The earth's magnetic field vector, \bar{H}_m , is contained in the yz -plane at a dip or inclination angle, I (measured from the horizontal).

A resultant wave, \bar{E}_t , transmitted into the model ionosphere ($z > 0$), figure 2, is then assumed to have the form

$$E_t = |\bar{E}_t| \exp \left[i \left(\omega t - \frac{\omega}{c} \eta D \right) \right], \quad (3)$$

where in the model plasma

$$\eta D = x \sin \phi_i \sin \phi_a + y \sin \phi_i \cos \phi_a + z \zeta, \quad (4)$$

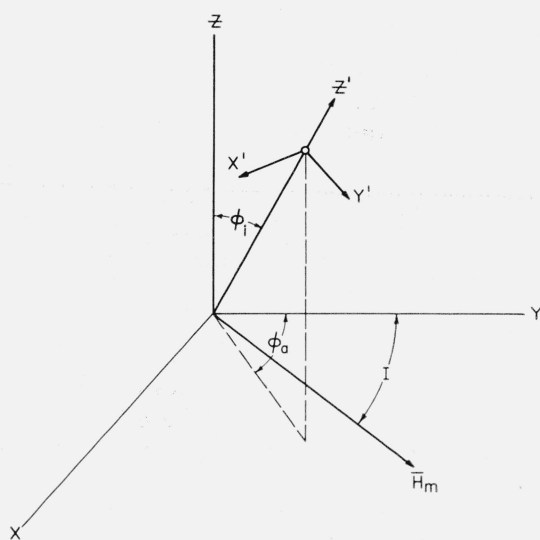


FIGURE 1. Coordinate systems.

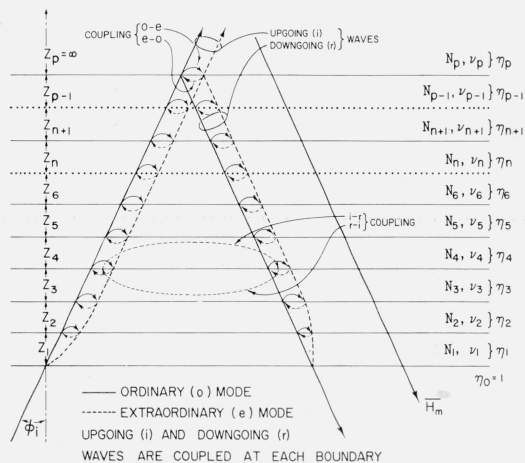


FIGURE 2. Structure of the flexible plasma model, illustrating ordinary and extraordinary modes of propagation, coupled at the boundaries.

Each z_n , $n=1, 2, 3, \dots, p$, becomes smaller as the number of slabs, p , is increased, until a stable reflection is obtained. z_p is always infinite, where each N_n, ν_n corresponds to median values of the intervals, z_n , respectively of the particular profiles under investigation.

in which ζ is in general a complex number, the value of which will depend upon altitude, z , $\zeta = \zeta(z)$.

The quantity ζ is determined by a simultaneous solution of Maxwell's equations,³

$$\bar{\nabla} \times \bar{E} + \mu_0 \frac{\partial \bar{H}}{\partial t} = 0, \quad (5)$$

$$\bar{\nabla} \times \bar{H} - \bar{J} - \epsilon_0 \frac{\partial \bar{E}}{\partial t} = 0, \quad (6)$$

and the equation of motion of the electron,

$$m \frac{d\bar{V}}{dt} + m g \bar{V} + \mu_0 e \left(\bar{V} \times \bar{H}_m \right) + e \bar{E} = 0, \quad (7)$$

with the electric field, \bar{E} , volts/meter; the magnetic field, \bar{H} , ampere-turns/meter; the convection current density, $\bar{J} = -N e \bar{V}$; N electrons per cubic meter (electrons/cm³ is frequently employed to describe N) with charge, e ; mass, m ; and vector velocity, \bar{V} , where μ_0 and ϵ_0 are the permeability and permittivity of space respectively. The constant real collision frequency, $g \sim \nu$, of the classical magneto-ionic theory is employed initially, but will be generalized to a complex, frequency-dependent parameter, g , during the course of the paper.

The vectors \bar{V} and \bar{H} can be eliminated, whereupon it can be concluded that the field \bar{E} exists in the medium if a quartic in ζ is satisfied [Booker, 1934, Jöhler and Walters, 1960]⁴

$$a_4 \zeta^4 + a_3 \zeta^3 + a_2 \zeta^2 + a_1 \zeta + a_0 = 0, \quad (8)$$

where

$$a_0 = (\sin^2 \phi_i - 1)^2 \left[1 - \frac{s}{s^2 - h^2} \right] + (\sin^2 \phi_i - 1) \left[\frac{1}{s} + \frac{s-2}{s^2 - h^2} + \frac{a_L^2 h_T^2}{s(s^2 - h^2)} \right] + \frac{s-1}{s(s^2 - h^2)}, \quad (9)$$

$$a_1 = 2 \frac{h_L h_T a_L}{s(s^2 - h^2)} (\sin^2 \phi_i - 1), \quad (10)$$

$$a_2 = \left\{ 2 \left[1 - \frac{s}{s^2 - h^2} \right] + \frac{h_L^2}{s(s^2 - h^2)} \right\} (\sin^2 \phi_i - 1) + \frac{h_T^2 a_L^2}{s(s^2 - h^2)} + \frac{s-2}{s^2 - h^2} + \frac{1}{s}, \quad (11)$$

$$a_3 = 2 \frac{h_L h_T a_L}{s(s^2 - h^2)} - a_1 \sec^2 \phi_i, \quad (12)$$

$$a_4 = 1 - \frac{s^2 - h_L^2}{s(s^2 - h^2)}, \quad (13)$$

$$s = \frac{\omega^2}{\omega_N^2} \left[1 - i \frac{\nu}{\omega} \right], \quad (14)$$

where $\nu = \nu_n$, the collision frequency of the particular slab, n , figure 2, under investigation,⁵

$$h = \frac{\omega_H \omega}{\omega_N^2}, \quad (15)$$

$$h_L = -h \sin I, \quad (16)$$

$$h_T = h \cos I, \quad (17)$$

$$a_L = \sin \phi_i \cos \phi_a, \quad a_T = \sin \phi_i \sin \phi_a, \quad (18)$$

$$a = \sin \phi_i \quad (19)$$

$$\omega_N^2 = N e^2 / \kappa m, \quad (20)$$

³ Rationalized mks units are employed.

⁴ See eq (21) of paper by Jöhler and Walters [1960].

⁵ In previous papers [Jöhler and Walters, 1960; Jöhler, 1961a] $\omega_L = \omega_H$, $\omega_{cr}^2 = \omega_N^2$.

where $N=N_n$ the electron density of the particular slab, n , figure 2, under investigation,

$$\omega_H = \mu_0 e H_m / m, \text{ the gyrofrequency,}^5 \quad (21)$$

$$\kappa = 1/c^2 \mu_0 = \epsilon_0. \quad (22)$$

Two pairs of roots, ζ , can be found by previously described methods [Jöhler and Walters 1960] where each root represents either an ordinary or an extraordinary, upgoing or downgoing wave propagated in the model plasma.

The detailed structure of the flexible plasma model is illustrated, figure 2, as a stack of plasma slabs of arbitrary thickness (but consistent with computation efficiency) z_n except the topmost slab of thickness $z_p = \infty$. The number of such slabs, p , is also quite flexible, since the notion is implied in this analysis that the measured electron density-altitude and collision frequency-altitude profiles can be approximated to any desired accuracy by decreasing z_n and increasing p simultaneously until a stable reflection process is obtained.

A constant electron density and collision frequency with respect to altitude, z , is of course assumed for each slab, z_n ; and associated with each such slab a set of four roots, $\zeta = \zeta_n$, is found to exist. Two of the roots will exhibit a negative imaginary, $\text{Im } \zeta$ negative, corresponding to an upgoing wave ($+z$ direction, figs. 1 and 2) and two of these roots will correspond to a positive imaginary, $\text{Im } \zeta$ positive, corresponding to a downgoing ($-z$ direction figs. 1 and 2). Except for the topmost slab, it is necessary to consider both upgoing and downgoing waves in this analysis, whereas in previous analysis [Jöhler and Walters, 1960] only the upgoing waves were considered. The previous analysis implied that the upgoing waves were completely transmitted or absorbed before another reflection could occur, and all reflections occurred at the first boundary. Such a model must be applied with considerable caution. But the restrictions of such a model are removed by this analysis and, indeed, the sharply bounded model can be replaced in the limit by a continuum in which the electron density and collision frequency vary with altitude as a smooth but quite arbitrary function. This of course permits the use of the detailed measured profiles of the lower ionosphere.

The treatment of a continuously varying medium by approximating the medium with one or more slabs of uniform composition has been utilized by many authors [Hines, 1951; Ferraro and Gibbons, 1959; Brekhovskikh, 1960; Wait, 1960 and 1961]. Such methods are exploited in this paper and carried to the limit, such that the number of slabs, p , for each calculation depends upon the computation precision required and the particular values of the electric and geometric parameters.

It is, however, necessary to distinguish between ordinary and extraordinary modes of propagation for both the upgoing and downgoing waves. This is accomplished by an examination of the form of the index of refraction function with respect to frequency and altitude (or electron density and collision frequency which varies with respect to altitude). Thus, the index of refraction, η (as defined by eq (4)),

$$\eta^2 = \zeta^2 + \sin^2 \phi_i, \quad (23)$$

is detailed for each frequency and slab z_n , $\eta = \eta_n$, and the upgoing ordinary and extraordinary $\eta_{i,o,e}^{(n)}$ and the downgoing $\eta_{r,o,e}^{(n)}$ ordinary and extraordinary function continuity is examined in detail as a function of frequency to determine the crossover point of the functions⁶ for each slab or electron density under consideration. The $\text{Re } \eta$ was employed in this analysis. Thus, above the crossover point the ordinary wave was considered to be the greater of the two roots $\text{Re } \eta_o > \text{Re } \eta_e$ and below the crossover point the ordinary wave was considered to be the lesser of the two roots, $\text{Re } \eta_o < \text{Re } \eta_e$. At precisely the crossover point, the two, of course, are identical, $\eta_o = \eta_e$ which point, for examples with low electron density examined in this analysis, was found to be below the critical frequency, $f_N = \omega_N / 2\pi$. The absolute distinction between the two modes of propagation remains quite arbitrary as in previous analysis [Jöhler and Walters, 1960], but the analysis must be consistent between each slab and consistent within each slab for upgoing and downgoing waves.

⁶ Index of refraction, η , continuity analysis to determine crossover was coded as a logic routine for the CDC-1604 computer as was the whole of this analysis.

the E_x field,

$$E_{x^1} \cos \phi_a + E_{y^1} \cos \phi_a \sin \phi_a + E_{x^1 r} \cos \phi_a - E_{y^1 r} \cos \phi_a \sin \phi_a = Q_{io}^{(1)} E_{yio}^{(1)} + Q_{ie}^{(1)} E_{yie}^{(1)} + Q_{ro}^{(1)} E_{yro}^{(1)} + Q_{re}^{(1)} E_{yre}^{(1)}$$

$$Q_{io}^{(1)} E_{yio}^{(1)} \exp[-i \frac{\omega}{c} z_1 \zeta_{io}^{(1)}] + Q_{ie}^{(1)} E_{yie}^{(1)} \exp[-i \frac{\omega}{c} z_1 \zeta_{ie}^{(1)}] + Q_{ro}^{(1)} E_{yro}^{(1)} \exp[-i \frac{\omega}{c} z_1 \zeta_{ro}^{(1)}] + Q_{re}^{(1)} E_{yre}^{(1)} \exp[-i \frac{\omega}{c} z_1 \zeta_{re}^{(1)}] = Q_{io}^{(2)} E_{yio}^{(2)} + Q_{ie}^{(2)} E_{yie}^{(2)} + Q_{ro}^{(2)} E_{yro}^{(2)} + Q_{re}^{(2)} E_{yre}^{(2)}$$

$$Q_{io}^{(2)} E_{yio}^{(2)} \exp[-i \frac{\omega}{c} z_2 \zeta_{io}^{(2)}] + Q_{ie}^{(2)} E_{yie}^{(2)} \exp[-i \frac{\omega}{c} z_2 \zeta_{ie}^{(2)}] + Q_{ro}^{(2)} E_{yro}^{(2)} \exp[-i \frac{\omega}{c} z_2 \zeta_{ro}^{(2)}] + Q_{re}^{(2)} E_{yre}^{(2)} \exp[-i \frac{\omega}{c} z_2 \zeta_{re}^{(2)}] = Q_{io}^{(3)} E_{yio}^{(3)} + Q_{ie}^{(3)} E_{yie}^{(3)} + Q_{ro}^{(3)} E_{yro}^{(3)} + Q_{re}^{(3)} E_{yre}^{(3)}$$

$$Q_{io}^{(p-1)} E_{yio}^{(p-1)} \exp[-i \frac{\omega}{c} z_{p-1} \zeta_{io}^{(p-1)}] + Q_{ie}^{(p-1)} E_{yie}^{(p-1)} \exp[-i \frac{\omega}{c} z_{p-1} \zeta_{ie}^{(p-1)}] + Q_{ro}^{(p-1)} E_{yro}^{(p-1)} \exp[-i \frac{\omega}{c} z_{p-1} \zeta_{ro}^{(p-1)}] + Q_{re}^{(p-1)} E_{yre}^{(p-1)} \exp[-i \frac{\omega}{c} z_{p-1} \zeta_{re}^{(p-1)}] = Q_{io}^{(p)} E_{yio}^{(p)} + Q_{ie}^{(p)} E_{yie}^{(p)}$$

(24)

the E_y field,

$$-E_{x^1} \sin \phi_a + E_{y^1} \cos \phi_a \cos \phi_a - E_{x^1 r} \sin \phi_a - E_{y^1 r} \cos \phi_a \cos \phi_a = E_{yio}^{(1)} + E_{yie}^{(1)} + E_{yro}^{(1)} + E_{yre}^{(1)}$$

$$E_{yio}^{(1)} \exp[-i \frac{\omega}{c} z_1 \zeta_{io}^{(1)}] + E_{yie}^{(1)} \exp[-i \frac{\omega}{c} z_1 \zeta_{ie}^{(1)}] + E_{yro}^{(1)} \exp[-i \frac{\omega}{c} z_1 \zeta_{ro}^{(1)}] + E_{yre}^{(1)} \exp[-i \frac{\omega}{c} z_1 \zeta_{re}^{(1)}] = E_{yio}^{(2)} + E_{yie}^{(2)} + E_{yro}^{(2)} + E_{yre}^{(2)}$$

$$E_{yio}^{(2)} \exp[-i \frac{\omega}{c} z_2 \zeta_{io}^{(2)}] + E_{yie}^{(2)} \exp[-i \frac{\omega}{c} z_2 \zeta_{ie}^{(2)}] + E_{yro}^{(2)} \exp[-i \frac{\omega}{c} z_2 \zeta_{ro}^{(2)}] + E_{yre}^{(2)} \exp[-i \frac{\omega}{c} z_2 \zeta_{re}^{(2)}] = E_{yio}^{(3)} + E_{yie}^{(3)} + E_{yro}^{(3)} + E_{yre}^{(3)}$$

$$E_{yio}^{(p-1)} \exp[-i \frac{\omega}{c} z_{p-1} \zeta_{io}^{(p-1)}] + E_{yie}^{(p-1)} \exp[-i \frac{\omega}{c} z_{p-1} \zeta_{ie}^{(p-1)}] + E_{yro}^{(p-1)} \exp[-i \frac{\omega}{c} z_{p-1} \zeta_{ro}^{(p-1)}] + E_{yre}^{(p-1)} \exp[-i \frac{\omega}{c} z_{p-1} \zeta_{re}^{(p-1)}] = E_{yio}^{(p)} + E_{yie}^{(p)}$$

(25)

the H_x field,

$$E_{x^1} \cos \phi_a \sin \phi_a - E_{y^1} \cos \phi_a - E_{x^1 r} \cos \phi_a \sin \phi_a - E_{y^1 r} \cos \phi_a = [a_L P_{io}^{(1)} - \zeta_{io}^{(1)}] E_{yio}^{(1)} + [a_L P_{ie}^{(1)} - \zeta_{ie}^{(1)}] E_{yie}^{(1)} + [a_L P_{ro}^{(1)} - \zeta_{ro}^{(1)}] E_{yro}^{(1)} + [a_L P_{re}^{(1)} - \zeta_{re}^{(1)}] E_{yre}^{(1)}$$

$$[a_L P_{io}^{(1)} - \zeta_{io}^{(1)}] E_{yio}^{(1)} \exp[-i \frac{\omega}{c} z_1 \zeta_{io}^{(1)}] + [a_L P_{ie}^{(1)} - \zeta_{ie}^{(1)}] E_{yie}^{(1)} \exp[-i \frac{\omega}{c} z_1 \zeta_{ie}^{(1)}] + [a_L P_{ro}^{(1)} - \zeta_{ro}^{(1)}] E_{yro}^{(1)} \exp[-i \frac{\omega}{c} z_1 \zeta_{ro}^{(1)}] + [a_L P_{re}^{(1)} - \zeta_{re}^{(1)}] E_{yre}^{(1)} \exp[-i \frac{\omega}{c} z_1 \zeta_{re}^{(1)}] = [a_L P_{io}^{(2)} - \zeta_{io}^{(2)}] E_{yio}^{(2)} + [a_L P_{ie}^{(2)} - \zeta_{ie}^{(2)}] E_{yie}^{(2)} + [a_L P_{ro}^{(2)} - \zeta_{ro}^{(2)}] E_{yro}^{(2)} + [a_L P_{re}^{(2)} - \zeta_{re}^{(2)}] E_{yre}^{(2)}$$

$$[a_L P_{io}^{(2)} - \zeta_{io}^{(2)}] E_{yio}^{(2)} \exp[-i \frac{\omega}{c} z_2 \zeta_{io}^{(2)}] + [a_L P_{ie}^{(2)} - \zeta_{ie}^{(2)}] E_{yie}^{(2)} \exp[-i \frac{\omega}{c} z_2 \zeta_{ie}^{(2)}] + [a_L P_{ro}^{(2)} - \zeta_{ro}^{(2)}] E_{yro}^{(2)} \exp[-i \frac{\omega}{c} z_2 \zeta_{ro}^{(2)}] + [a_L P_{re}^{(2)} - \zeta_{re}^{(2)}] E_{yre}^{(2)} \exp[-i \frac{\omega}{c} z_2 \zeta_{re}^{(2)}] = [a_L P_{io}^{(3)} - \zeta_{io}^{(3)}] E_{yio}^{(3)} + [a_L P_{ie}^{(3)} - \zeta_{ie}^{(3)}] E_{yie}^{(3)} + [a_L P_{ro}^{(3)} - \zeta_{ro}^{(3)}] E_{yro}^{(3)} + [a_L P_{re}^{(3)} - \zeta_{re}^{(3)}] E_{yre}^{(3)}$$

$$[a_L P_{io}^{(p-1)} - \zeta_{io}^{(p-1)}] E_{yio}^{(p-1)} \exp[-i \frac{\omega}{c} z_{p-1} \zeta_{io}^{(p-1)}] + [a_L P_{ie}^{(p-1)} - \zeta_{ie}^{(p-1)}] E_{yie}^{(p-1)} \exp[-i \frac{\omega}{c} z_{p-1} \zeta_{ie}^{(p-1)}] + [a_L P_{ro}^{(p-1)} - \zeta_{ro}^{(p-1)}] E_{yro}^{(p-1)} \exp[-i \frac{\omega}{c} z_{p-1} \zeta_{ro}^{(p-1)}] + [a_L P_{re}^{(p-1)} - \zeta_{re}^{(p-1)}] E_{yre}^{(p-1)} \exp[-i \frac{\omega}{c} z_{p-1} \zeta_{re}^{(p-1)}] = [a_L P_{io}^{(p)} - \zeta_{io}^{(p)}] E_{yio}^{(p)} + [a_L P_{ie}^{(p)} - \zeta_{ie}^{(p)}] E_{yie}^{(p)}$$

(26)

the H_y field,

$$E_{x^1} \cos \phi_a \cos \phi_a + E_{y^1} \sin \phi_a - E_{x^1 r} \cos \phi_a \cos \phi_a + E_{y^1 r} \sin \phi_a = [\zeta_{io}^{(1)} Q_{io}^{(1)} - a_T P_{io}^{(1)}] E_{yio}^{(1)} + [\zeta_{ie}^{(1)} Q_{ie}^{(1)} - a_T P_{ie}^{(1)}] E_{yie}^{(1)} + [\zeta_{ro}^{(1)} Q_{ro}^{(1)} - a_T P_{ro}^{(1)}] E_{yro}^{(1)} + [\zeta_{re}^{(1)} Q_{re}^{(1)} - a_T P_{re}^{(1)}] E_{yre}^{(1)}$$

$$[\zeta_{io}^{(1)} Q_{io}^{(1)} - a_T P_{io}^{(1)}] E_{yio}^{(1)} \exp[-i \frac{\omega}{c} z_1 \zeta_{io}^{(1)}] + [\zeta_{ie}^{(1)} Q_{ie}^{(1)} - a_T P_{ie}^{(1)}] E_{yie}^{(1)} \exp[-i \frac{\omega}{c} z_1 \zeta_{ie}^{(1)}] + [\zeta_{ro}^{(1)} Q_{ro}^{(1)} - a_T P_{ro}^{(1)}] E_{yro}^{(1)} \exp[-i \frac{\omega}{c} z_1 \zeta_{ro}^{(1)}] + [\zeta_{re}^{(1)} Q_{re}^{(1)} - a_T P_{re}^{(1)}] E_{yre}^{(1)} \exp[-i \frac{\omega}{c} z_1 \zeta_{re}^{(1)}] = [\zeta_{io}^{(2)} Q_{io}^{(2)} - a_T P_{io}^{(2)}] E_{yio}^{(2)} + [\zeta_{ie}^{(2)} Q_{ie}^{(2)} - a_T P_{ie}^{(2)}] E_{yie}^{(2)} + [\zeta_{ro}^{(2)} Q_{ro}^{(2)} - a_T P_{ro}^{(2)}] E_{yro}^{(2)} + [\zeta_{re}^{(2)} Q_{re}^{(2)} - a_T P_{re}^{(2)}] E_{yre}^{(2)}$$

$$[\zeta_{io}^{(2)} Q_{io}^{(2)} - a_T P_{io}^{(2)}] E_{yio}^{(2)} \exp[-i \frac{\omega}{c} z_2 \zeta_{io}^{(2)}] + [\zeta_{ie}^{(2)} Q_{ie}^{(2)} - a_T P_{ie}^{(2)}] E_{yie}^{(2)} \exp[-i \frac{\omega}{c} z_2 \zeta_{ie}^{(2)}] + [\zeta_{ro}^{(2)} Q_{ro}^{(2)} - a_T P_{ro}^{(2)}] E_{yro}^{(2)} \exp[-i \frac{\omega}{c} z_2 \zeta_{ro}^{(2)}] + [\zeta_{re}^{(2)} Q_{re}^{(2)} - a_T P_{re}^{(2)}] E_{yre}^{(2)} \exp[-i \frac{\omega}{c} z_2 \zeta_{re}^{(2)}] = [\zeta_{io}^{(3)} Q_{io}^{(3)} - a_T P_{io}^{(3)}] E_{yio}^{(3)} + [\zeta_{ie}^{(3)} Q_{ie}^{(3)} - a_T P_{ie}^{(3)}] E_{yie}^{(3)} + [\zeta_{ro}^{(3)} Q_{ro}^{(3)} - a_T P_{ro}^{(3)}] E_{yro}^{(3)} + [\zeta_{re}^{(3)} Q_{re}^{(3)} - a_T P_{re}^{(3)}] E_{yre}^{(3)}$$

$$[\zeta_{io}^{(p-1)} Q_{io}^{(p-1)} - a_T P_{io}^{(p-1)}] E_{yio}^{(p-1)} \exp[-i \frac{\omega}{c} z_{p-1} \zeta_{io}^{(p-1)}] + [\zeta_{ie}^{(p-1)} Q_{ie}^{(p-1)} - a_T P_{ie}^{(p-1)}] E_{yie}^{(p-1)} \exp[-i \frac{\omega}{c} z_{p-1} \zeta_{ie}^{(p-1)}] + [\zeta_{ro}^{(p-1)} Q_{ro}^{(p-1)} - a_T P_{ro}^{(p-1)}] E_{yro}^{(p-1)} \exp[-i \frac{\omega}{c} z_{p-1} \zeta_{ro}^{(p-1)}] + [\zeta_{re}^{(p-1)} Q_{re}^{(p-1)} - a_T P_{re}^{(p-1)}] E_{yre}^{(p-1)} \exp[-i \frac{\omega}{c} z_{p-1} \zeta_{re}^{(p-1)}] = [\zeta_{io}^{(p)} Q_{io}^{(p)} - a_T P_{io}^{(p)}] E_{yio}^{(p)} + [\zeta_{ie}^{(p)} Q_{ie}^{(p)} - a_T P_{ie}^{(p)}] E_{yie}^{(p)}$$

(27)

the H_z field,

$$-E_{x^1} \sin \phi_a - E_{x^1 r} \sin \phi_a = (a_T - a_L Q_{io}^{(1)}) E_{yio}^{(1)} + (a_T - a_L Q_{ie}^{(1)}) E_{yie}^{(1)} + (a_T - a_L Q_{ro}^{(1)}) E_{yro}^{(1)} + (a_T - a_L Q_{re}^{(1)}) E_{yre}^{(1)}$$

$$(a_T - a_L Q_{io}^{(1)}) E_{yio}^{(1)} \exp[-i \frac{\omega}{c} z_1 \zeta_{io}^{(1)}] + (a_T - a_L Q_{ie}^{(1)}) E_{yie}^{(1)} \exp[-i \frac{\omega}{c} z_1 \zeta_{ie}^{(1)}] + (a_T - a_L Q_{ro}^{(1)}) E_{yro}^{(1)} \exp[-i \frac{\omega}{c} z_1 \zeta_{ro}^{(1)}] + (a_T - a_L Q_{re}^{(1)}) E_{yre}^{(1)} \exp[-i \frac{\omega}{c} z_1 \zeta_{re}^{(1)}] = (a_T - a_L Q_{io}^{(2)}) E_{yio}^{(2)} + (a_T - a_L Q_{ie}^{(2)}) E_{yie}^{(2)} + (a_T - a_L Q_{ro}^{(2)}) E_{yro}^{(2)} + (a_T - a_L Q_{re}^{(2)}) E_{yre}^{(2)}$$

$$(a_T - a_L Q_{io}^{(2)}) E_{yio}^{(2)} \exp[-i \frac{\omega}{c} z_2 \zeta_{io}^{(2)}] + (a_T - a_L Q_{ie}^{(2)}) E_{yie}^{(2)} \exp[-i \frac{\omega}{c} z_2 \zeta_{ie}^{(2)}] + (a_T - a_L Q_{ro}^{(2)}) E_{yro}^{(2)} \exp[-i \frac{\omega}{c} z_2 \zeta_{ro}^{(2)}] + (a_T - a_L Q_{re}^{(2)}) E_{yre}^{(2)} \exp[-i \frac{\omega}{c} z_2 \zeta_{re}^{(2)}] = (a_T - a_L Q_{io}^{(3)}) E_{yio}^{(3)} + (a_T - a_L Q_{ie}^{(3)}) E_{yie}^{(3)} + (a_T - a_L Q_{ro}^{(3)}) E_{yro}^{(3)} + (a_T - a_L Q_{re}^{(3)}) E_{yre}^{(3)}$$

$$(a_T - a_L Q_{io}^{(p-1)}) E_{yio}^{(p-1)} \exp[-i \frac{\omega}{c} z_{p-1} \zeta_{io}^{(p-1)}] + (a_T - a_L Q_{ie}^{(p-1)}) E_{yie}^{(p-1)} \exp[-i \frac{\omega}{c} z_{p-1} \zeta_{ie}^{(p-1)}] + (a_T - a_L Q_{ro}^{(p-1)}) E_{yro}^{(p-1)} \exp[-i \frac{\omega}{c} z_{p-1} \zeta_{ro}^{(p-1)}] + (a_T - a_L Q_{re}^{(p-1)}) E_{yre}^{(p-1)} \exp[-i \frac{\omega}{c} z_{p-1} \zeta_{re}^{(p-1)}] = (a_T - a_L Q_{io}^{(p)}) E_{yio}^{(p)} + (a_T - a_L Q_{ie}^{(p)}) E_{yie}^{(p)}$$

(28)

3. Determination of the Reflection and Transmission Coefficients

The reflection and transmission coefficients are determined by the boundary conditions which express the principle of continuity of the tangential \overline{E} and \overline{H} fields and the normal \overline{H} fields at each boundary, figures 1, 2, of the model plasma. These fields are equated immediately above and immediately below each boundary. (See eqs. 24 to 28 on p. 85.) where

$$Q = \frac{E_x}{E_y}, \quad (29)$$

$$P = \frac{E_z}{E_y}, \quad (30)$$

and the subscripts io, ie, ro, re refer to upgoing ordinary, upgoing extraordinary, downgoing ordinary, and downgoing extraordinary modes of propagation. The superscripts $n=1, 2, 3, \dots, p-1$, and p refer to the particular medium, figure 2, under consideration, with corresponding values N, ν , which together with the magnetic parameters, H_m, ϕ_a, I , and the angle of incidence, ϕ_i , determine the index of refraction, (23). The process is of course continued until convergence is obtained on the particular profiles of electron density and collision frequency under investigation. Notice that the topmost slab, $z_p = \infty, n=p$, has only two terms representing the two upgoing waves. The downgoing waves do not exist since the topmost slab is assumed to be of infinite, homogeneous extent. However, this analysis can readily determine the transmission coefficient of a finite slab of plasma with an $N(h) = N(z)$, and $\nu(h) = \nu(z)$ profile which varies with altitude, z , simply by replacing the last two terms of eqs (24 to 28) with

$$\begin{aligned} & E_{x't} \cos \phi_a + E_{y't} \cos \phi_i \sin \phi_a, \\ & -E_{x't} \sin \phi_a + E_{y't} \cos \phi_i \cos \phi_a, \\ & E_{x't} \cos \phi_i \sin \phi_a - E_{y't} \cos \phi_a, \\ & E_{x't} \cos \phi_i \cos \phi_a + E_{y't} \sin \phi_a, \\ & -E_{x't} \sin \phi_i, \end{aligned} \quad (31)$$

respectively, where $E_{x't}, E_{y't}$, are the components of the transmitted fields.

The reflection, T , and transmission T', U , coefficients can now be defined

$$\begin{aligned} T_{ee} &= \frac{E_{y'r}}{E_{y'i}} & T'_{ee} &= \frac{E_{y't}}{E_{y'i}} & U_{eio}^{(n)} &= \frac{E_{y'io}^{(n)}}{E_{y'i}} & U_{e\tau o}^{(n)} &= \frac{E_{y'ro}^{(n)}}{E_{y'i}} \\ T_{em} &= \frac{E_{x'r}}{E_{y'i}} & T'_{em} &= \frac{E_{x't}}{E_{y'i}} & U_{mio}^{(n)} &= \frac{E_{y'io}^{(n)}}{E_{x'i}} & U_{m\tau o}^{(n)} &= \frac{E_{y'ro}^{(n)}}{E_{x'i}} \\ T_{me} &= \frac{E_{y'r}}{E_{x'i}} & T'_{me} &= \frac{E_{y't}}{E_{x'i}} & U_{eie}^{(n)} &= \frac{E_{y'ie}^{(n)}}{E_{x'i}} & U_{e\tau e}^{(n)} &= \frac{E_{y're}^{(n)}}{E_{x'i}} \\ T_{mm} &= \frac{E_{x'r}}{E_{x'i}} & T'_{mm} &= \frac{E_{x't}}{E_{x'i}} & U_{mie}^{(n)} &= \frac{E_{y'ie}^{(n)}}{E_{x'i}} & U_{m\tau e}^{(n)} &= \frac{E_{y're}^{(n)}}{E_{x'i}} \end{aligned} \quad (32)$$

where, figure 2, $n=1, 2, 3, \dots, p-1, p$, and the four T 's are defined as a transmission coefficient into a topmost slab of infinite extent, z , and zero electron density, $N=0, \eta_p = \eta_o = 1$.

The reflection coefficients, $T_{ee}, T_{em}, T_{me}, T_{mm}$, describe the reflection into the region below the model plasma, $z < 0$. Thus, T_{ee} refers to vertical electric polarization of the incident wave and a corresponding vertical electric polarization of the reflected wave. T_{em} refers to the generation of the abnormal component (horizontal electric polarization) by the incident vertical electric wave. Similarly, T_{mm} refers to vertical magnetic incident wave and vertical magnetic reflected wave, and T_{me} refers to a corresponding abnormal component (horizontal magnetic).

The transmission coefficients, U , refer to transmission at the particular point in the ionosphere under investigation to which the wave has penetrated. There are thus four modes of

propagation and two polarizations and hence eight types of transmission coefficients: upgoing and downgoing, ordinary and extraordinary, vertical electric and vertical magnetic.

Thus, the nature of the wave reflected from the plasma, the nature of the wave transmitted through the plasma, and indeed the nature of the wave progressing within the plasma are completely described by the coefficients determined by this analysis.

Four of the boundary conditions (24 to 27) result in the matrix equation

$$\begin{bmatrix}
 a_{1,1} & a_{1,2} & a_{1,3} & a_{1,4} & a_{1,5} & a_{1,6} \\
 a_{2,3} & a_{2,4} & a_{2,5} & a_{2,6} & a_{2,7} & a_{2,8} & a_{2,9} & a_{2,10} \\
 a_{3,7} & a_{3,8} & a_{3,9} & a_{3,10} & a_{3,11} & a_{3,12} & a_{3,13} & a_{3,14} \\
 \dots & \dots & \dots & \dots & \dots & \dots & \dots & \dots \\
 a_{p,p+4} & \dots & \dots & \dots & \dots & \dots & \dots & a_{p,p+9} \\
 \\
 b_{1,1} & b_{1,2} & b_{1,3} & b_{1,4} & b_{1,5} & b_{1,6} \\
 b_{2,3} & b_{2,4} & b_{2,5} & b_{2,6} & b_{2,7} & b_{2,8} & b_{2,9} & b_{2,10} \\
 b_{3,7} & b_{3,8} & b_{3,9} & b_{3,10} & b_{3,11} & b_{3,12} & b_{3,13} & b_{3,14} \\
 \dots & \dots & \dots & \dots & \dots & \dots & \dots & \dots \\
 b_{p,p+4} & \dots & \dots & \dots & \dots & \dots & \dots & b_{p,p+9} \\
 \\
 c_{1,1} & c_{1,2} & c_{1,3} & c_{1,4} & c_{1,5} & c_{1,6} \\
 c_{2,3} & c_{2,4} & c_{2,5} & c_{2,6} & c_{2,7} & c_{2,8} & c_{2,9} & c_{2,10} \\
 c_{3,7} & c_{3,8} & c_{3,9} & c_{3,10} & c_{3,11} & c_{3,12} & c_{3,13} & c_{3,14} \\
 \dots & \dots & \dots & \dots & \dots & \dots & \dots & \dots \\
 c_{p,p+4} & \dots & \dots & \dots & \dots & \dots & \dots & c_{p,p+9} \\
 \\
 d_{1,1} & d_{1,2} & d_{1,3} & d_{1,4} & d_{1,5} & d_{1,6} \\
 d_{2,3} & d_{2,4} & d_{2,5} & d_{2,6} & d_{2,7} & d_{2,8} & d_{2,9} & d_{2,10} \\
 d_{3,7} & d_{3,8} & d_{3,9} & d_{3,10} & d_{3,11} & d_{3,12} & d_{3,13} & d_{3,14} \\
 \dots & \dots & \dots & \dots & \dots & \dots & \dots & \dots \\
 d_{p,p+4} & \dots & \dots & \dots & \dots & \dots & \dots & d_{p,p+9}
 \end{bmatrix}
 +
 \begin{bmatrix}
 T_{em}, T_{mm} \\
 T_{ee}, T_{me} \\
 U_{eio}^{(1)}, U_{mio}^{(1)} \\
 U_{eie}^{(1)}, U_{mie}^{(1)} \\
 U_{ero}^{(1)}, U_{mro}^{(1)} \\
 U_{ere}^{(1)}, U_{mre}^{(1)} \\
 U_{eio}^{(2)}, U_{mio}^{(2)} \\
 U_{eie}^{(2)}, U_{mie}^{(2)} \\
 U_{ero}^{(2)}, U_{mro}^{(2)} \\
 U_{ere}^{(2)}, U_{mre}^{(2)} \\
 U_{eio}^{(3)}, U_{mio}^{(3)} \\
 \dots \\
 \dots \\
 U_{eio}^{(p-1)}, U_{mio}^{(p-1)} \\
 U_{eie}^{(p-1)}, U_{mie}^{(p-1)} \\
 U_{ero}^{(p-1)}, U_{mro}^{(p-1)} \\
 U_{ere}^{(p-1)}, U_{mre}^{(p-1)} \\
 U_{eio}^{(p)}, U_{mio}^{(p)} \\
 U_{eie}^{(p)}, U_{mie}^{(p)}
 \end{bmatrix}
 \begin{bmatrix}
 a_o, e', a_o, m \\
 \\
 b_o, e', b_o, m \\
 \\
 c_o, e', c_o, m \\
 \\
 d_o, e', d_o, m
 \end{bmatrix}
 = 0, \tag{33}$$

Rearrangement of the matrix, such that zeros do not appear on the diagonal, $a_{1,1}$ to $d_{p,p+9}$, results in a matrix which can be solved by the previously described methods [Johler and Walters, 1960]. (Note that the second subscript of the last term of each group is $p+9$ instead of $p+11$ since the topmost slab contains only the ordinary and extraordinary upgoing waves.)

$$\begin{bmatrix}
 a_{1,1} & a_{1,2} & a_{1,3} & a_{1,4} & a_{1,5} & a_{1,6} \\
 b_{1,1} & b_{1,2} & b_{1,3} & b_{1,4} & b_{1,5} & b_{1,6} \\
 c_{1,1} & c_{1,2} & c_{1,3} & c_{1,4} & c_{1,5} & c_{1,6} \\
 d_{1,1} & d_{1,2} & d_{1,3} & d_{1,4} & d_{1,5} & d_{1,6} \\
 a_{2,3} & a_{2,4} & a_{2,5} & a_{2,6} & a_{2,7} & a_{2,8} & a_{2,9} & a_{2,10} \\
 b_{2,3} & b_{2,4} & b_{2,5} & b_{2,6} & b_{2,7} & b_{2,8} & b_{2,9} & b_{2,10} \\
 c_{2,3} & c_{2,4} & c_{2,5} & c_{2,6} & c_{2,7} & c_{2,8} & c_{2,9} & c_{2,10} \\
 d_{2,3} & d_{2,4} & d_{2,5} & d_{2,6} & d_{2,7} & d_{2,8} & d_{2,9} & d_{2,10} \\
 a_{3,7} & a_{3,8} & a_{3,9} & a_{3,10} & a_{3,11} & a_{3,12} & a_{3,13} & a_{3,14} \\
 b_{3,7} & b_{3,8} & b_{3,9} & b_{3,10} & b_{3,11} & b_{3,12} & b_{3,13} & b_{3,14} \\
 c_{3,7} & c_{3,8} & c_{3,9} & c_{3,10} & c_{3,11} & c_{3,12} & c_{3,13} & c_{3,14} \\
 d_{3,7} & d_{3,8} & d_{3,9} & d_{3,10} & d_{3,11} & d_{3,12} & d_{3,13} & d_{3,14} \\
 \dots & \dots & \dots & \dots & \dots & \dots & \dots & \dots \\
 a_{p,p+4} & \dots & \dots & \dots & \dots & \dots & \dots & a_{p,p+9} \\
 b_{p,p+4} & \dots & \dots & \dots & \dots & \dots & \dots & b_{p,p+9} \\
 c_{p,p+4} & \dots & \dots & \dots & \dots & \dots & \dots & c_{p,p+9} \\
 d_{p,p+4} & \dots & \dots & \dots & \dots & \dots & \dots & d_{p,p+9}
 \end{bmatrix}
 +
 \begin{bmatrix}
 T_{em}, T_{mm} \\
 T_{ee}, T_{me} \\
 U_{eio}^{(1)}, U_{mio}^{(1)} \\
 U_{eie}^{(1)}, U_{mie}^{(1)} \\
 U_{ero}^{(1)}, U_{mro}^{(1)} \\
 U_{ere}^{(1)}, U_{mre}^{(1)} \\
 U_{eio}^{(2)}, U_{mio}^{(2)} \\
 U_{eie}^{(2)}, U_{mie}^{(2)} \\
 U_{ero}^{(2)}, U_{mro}^{(2)} \\
 U_{ere}^{(2)}, U_{mre}^{(2)} \\
 \dots \\
 \dots \\
 U_{eio}^{(p-1)}, U_{mio}^{(p-1)} \\
 U_{eie}^{(p-1)}, U_{mie}^{(p-1)} \\
 U_{ero}^{(p-1)}, U_{mro}^{(p-1)} \\
 U_{ere}^{(p-1)}, U_{mre}^{(p-1)} \\
 U_{eio}^{(p)}, U_{mio}^{(p)} \\
 U_{eie}^{(p)}, U_{mie}^{(p)}
 \end{bmatrix}
 \begin{bmatrix}
 a_o e', a_o m \\
 b_o e', b_o m \\
 c_o e', c_o m \\
 d_o e', d_o m
 \end{bmatrix}
 = 0, \tag{34}$$

where

$$\begin{aligned}
 a_{1,1} &= \cos \phi_a & b_{1,1} &= -\sin \phi_a \\
 a_{1,2} &= -\cos \phi_1 \sin \phi_a & b_{1,2} &= -\cos \phi_i \cos \phi_a \\
 a_{1,3} &= -Q_{i_o}^{(1)} & b_{1,3} &= -1 \\
 a_{1,4} &= -Q_{i_e}^{(1)} & b_{1,4} &= -1 \\
 a_{1,5} &= -Q_{r_o}^{(1)} & b_{1,5} &= -1 \\
 a_{1,6} &= -Q_{r_e}^{(1)} & b_{1,6} &= -1 \\
 a_{2,3} &= -a_{1,3} \exp \left[-i \frac{\omega}{c} z_1 \zeta_{i_o}^{(1)} \right] & b_{2,3} &= \exp \left[-i \frac{\omega}{c} z_1 \zeta_{i_o}^{(1)} \right] \\
 a_{2,4} &= -a_{1,4} \exp \left[-i \frac{\omega}{c} z_1 \zeta_{i_e}^{(1)} \right] & b_{2,4} &= \exp \left[-i \frac{\omega}{c} z_1 \zeta_{i_e}^{(1)} \right] \\
 a_{2,5} &= -a_{1,5} \exp \left[-i \frac{\omega}{c} z_1 \zeta_{r_o}^{(1)} \right] & b_{2,5} &= \exp \left[-i \frac{\omega}{c} z_1 \zeta_{r_o}^{(1)} \right] \\
 a_{2,6} &= -a_{1,6} \exp \left[-i \frac{\omega}{c} z_1 \zeta_{r_e}^{(1)} \right] & b_{2,6} &= \exp \left[-i \frac{\omega}{c} z_1 \zeta_{r_e}^{(1)} \right] \\
 a_{2,7} &= -Q_{i_o}^{(2)} & b_{2,7} &= -1 \\
 a_{2,8} &= -Q_{i_e}^{(2)} & b_{2,8} &= -1 \\
 a_{2,9} &= -Q_{r_o}^{(2)} & b_{2,9} &= -1 \\
 a_{2,10} &= -Q_{r_e}^{(2)} & b_{2,10} &= -1 \\
 a_{3,7} &= -a_{2,7} \exp \left[-i \frac{\omega}{c} z_2 \zeta_{i_o}^{(2)} \right] & b_{3,7} &= \exp \left[-i \frac{\omega}{c} z_2 \zeta_{i_o}^{(2)} \right] \\
 a_{3,8} &= -a_{2,8} \exp \left[-i \frac{\omega}{c} z_2 \zeta_{i_e}^{(2)} \right] & b_{3,8} &= \exp \left[-i \frac{\omega}{c} z_2 \zeta_{i_e}^{(2)} \right] \\
 a_{3,9} &= -a_{2,9} \exp \left[-i \frac{\omega}{c} z_2 \zeta_{r_o}^{(2)} \right] & b_{3,9} &= \exp \left[-i \frac{\omega}{c} z_2 \zeta_{r_o}^{(2)} \right] \\
 a_{3,10} &= -a_{2,10} \exp \left[-i \frac{\omega}{c} z_2 \zeta_{r_e}^{(2)} \right] & b_{3,10} &= \exp \left[-i \frac{\omega}{c} z_2 \zeta_{r_e}^{(2)} \right] \\
 a_{3,11} &= -Q_{i_o}^{(3)} & b_{3,11} &= -1 \\
 a_{3,12} &= -Q_{i_e}^{(3)} & b_{3,12} &= -1 \\
 a_{3,13} &= -Q_{r_o}^{(3)} & b_{3,13} &= -1 \\
 a_{3,14} &= -Q_{r_e}^{(3)} & b_{3,14} &= -1 \\
 & \dots & & \dots \\
 a_{p,p+4} &= -a_{p-1,p+4} \exp \left[-i \frac{\omega}{c} z_{p-1} \zeta_{i_o}^{(p-1)} \right] & b_{p,p+4} &= \exp \left[-i \frac{\omega}{c} z_{p-1} \zeta_{i_o}^{(p-1)} \right] \\
 & \dots & & \dots \\
 a_{p,p+9} &= -Q_{i_e}^{(p)} & b_{p,p+9} &= -1
 \end{aligned}$$

$$c_{1,1} = -\cos \phi_i \sin \phi_a$$

$$d_{1,1} = -\cos \phi_i \cos \phi_a$$

$$c_{1,2} = -\cos \phi_a$$

$$d_{1,2} = \sin \phi_a$$

$$c_{1,3} = -[a_L P_{io}^{(1)} - \zeta_{io}^{(1)}]$$

$$d_{1,3} = -[\zeta_{io}^{(1)} Q_{io}^{(1)} - a_T P_{io}^{(1)}]$$

$$c_{1,4} = -[a_L P_{ie}^{(1)} - \zeta_{ie}^{(1)}]$$

$$d_{1,4} = -[\zeta_{ie}^{(1)} Q_{ie}^{(1)} - a_T P_{ie}^{(1)}]$$

$$c_{1,5} = -[a_L P_{ro}^{(1)} - \zeta_{ro}^{(1)}]$$

$$d_{1,5} = -[\zeta_{ro}^{(1)} Q_{ro}^{(1)} - a_T P_{ro}^{(1)}]$$

$$c_{1,6} = -[a_L P_{re}^{(1)} - \zeta_{re}^{(1)}]$$

$$d_{1,6} = -[\zeta_{re}^{(1)} Q_{re}^{(1)} - a_T P_{re}^{(1)}]$$

$$c_{2,3} = -c_{1,3} \exp \left[-i \frac{\omega}{c} z_1 \zeta_{io}^{(1)} \right]$$

$$d_{2,3} = -d_{1,3} \exp \left[-i \frac{\omega}{c} z_1 \zeta_{io}^{(1)} \right]$$

$$c_{2,4} = -c_{1,4} \exp \left[-i \frac{\omega}{c} z_1 \zeta_{ie}^{(1)} \right]$$

$$d_{2,4} = -d_{1,4} \exp \left[-i \frac{\omega}{c} z_1 \zeta_{ie}^{(1)} \right]$$

$$c_{2,5} = -c_{1,5} \exp \left[-i \frac{\omega}{c} z_1 \zeta_{ro}^{(1)} \right]$$

$$d_{2,5} = -d_{1,5} \exp \left[-i \frac{\omega}{c} z_1 \zeta_{ro}^{(1)} \right]$$

$$c_{2,6} = -c_{1,6} \exp \left[-i \frac{\omega}{c} z_1 \zeta_{re}^{(1)} \right]$$

$$d_{2,6} = -d_{1,6} \exp \left[-i \frac{\omega}{c} z_1 \zeta_{re}^{(1)} \right]$$

$$c_{2,7} = -[a_L P_{io}^{(2)} - \zeta_{io}^{(2)}]$$

$$d_{2,7} = -[\zeta_{io}^{(2)} Q_{io}^{(2)} - a_T P_{io}^{(2)}]$$

$$c_{2,8} = -[a_L P_{ie}^{(2)} - \zeta_{ie}^{(2)}]$$

$$d_{2,8} = -[\zeta_{ie}^{(2)} Q_{ie}^{(2)} - a_T P_{ie}^{(2)}]$$

$$c_{2,9} = -[a_L P_{ro}^{(2)} - \zeta_{ro}^{(2)}]$$

$$d_{2,9} = -[\zeta_{ro}^{(2)} Q_{ro}^{(2)} - a_T P_{ro}^{(2)}]$$

$$c_{2,10} = -[a_L P_{re}^{(2)} - \zeta_{re}^{(2)}]$$

$$d_{2,10} = -[\zeta_{re}^{(2)} Q_{re}^{(2)} - a_T P_{re}^{(2)}]$$

$$c_{3,7} = -c_{2,7} \exp \left[-i \frac{\omega}{c} z_2 \zeta_{io}^{(2)} \right]$$

$$d_{3,7} = -d_{2,7} \exp \left[-i \frac{\omega}{c} z_2 \zeta_{io}^{(2)} \right]$$

$$c_{3,8} = -c_{2,8} \exp \left[-i \frac{\omega}{c} z_2 \zeta_{ie}^{(2)} \right]$$

$$d_{3,8} = -d_{2,8} \exp \left[-i \frac{\omega}{c} z_2 \zeta_{ie}^{(2)} \right]$$

$$c_{3,9} = -c_{2,9} \exp \left[-i \frac{\omega}{c} z_2 \zeta_{ro}^{(2)} \right]$$

$$d_{3,9} = -d_{2,9} \exp \left[-i \frac{\omega}{c} z_2 \zeta_{ro}^{(2)} \right]$$

$$c_{3,10} = -c_{2,10} \exp \left[-i \frac{\omega}{c} z_2 \zeta_{re}^{(2)} \right]$$

$$d_{3,10} = -d_{2,10} \exp \left[-i \frac{\omega}{c} z_2 \zeta_{re}^{(2)} \right]$$

$$c_{3,11} = -[a_L P_{io}^{(3)} - \zeta_{io}^{(3)}]$$

$$d_{3,11} = -[\zeta_{io}^{(3)} Q_{io}^{(3)} - a_T P_{io}^{(3)}]$$

$$c_{3,12} = -[a_L P_{ie}^{(3)} - \zeta_{ie}^{(3)}]$$

$$d_{3,12} = -[\zeta_{ie}^{(3)} Q_{ie}^{(3)} - a_T P_{ie}^{(3)}]$$

$$c_{3,13} = -[a_L P_{ro}^{(3)} - \zeta_{ro}^{(3)}]$$

$$d_{3,13} = -[\zeta_{ro}^{(3)} Q_{ro}^{(3)} - a_T P_{ro}^{(3)}]$$

$$c_{3,14} = -[a_L P_{re}^{(3)} - \zeta_{re}^{(3)}]$$

$$d_{3,14} = -[\zeta_{re}^{(3)} Q_{re}^{(3)} - a_T P_{re}^{(3)}]$$

.....

.....

$$c_{p,p+4} = -c_{p-1,p+4} \exp \left[-i \frac{\omega}{c} z_{p-1} \zeta_{io}^{(p-1)} \right] \quad d_{p,p+4} = -d_{p-1,p+4} \exp \left[-i \frac{\omega}{c} z_{p-1} \zeta_{io}^{(p-1)} \right]$$

.....

.....

$$c_{p,p+9} = -[a_L P_{ie}^{(p)} - \zeta_{ie}^{(p)}]$$

$$d_{p,p+9} = -[\zeta_{ie}^{(p)} Q_{ie}^{(p)} - a_T P_{ie}^{(p)}]$$

$$\begin{aligned}
a_{oe} &= \cos \phi_i \sin \phi_a & a_{om} &= \cos \phi_a \\
b_{oe} &= \cos \phi_i \cos \phi_a & b_{om} &= -\sin \phi_a \\
c_{oe} &= -\cos \phi_a & c_{om} &= \cos \phi_i \sin \phi_a \\
d_{oe} &= \sin \phi_a & d_{om} &= \cos \phi_i \cos \phi_a.
\end{aligned}$$

The analytic expressions for the complex numbers, $P_{io}^{(n)}$, $P_{ie}^{(n)}$, $P_{ro}^{(n)}$, $P_{re}^{(n)}$, $Q_{io}^{(n)}$, $Q_{ie}^{(n)}$, $Q_{ro}^{(n)}$, $Q_{re}^{(n)}$ can be derived from the definitions (29, 30) by a simultaneous solution of Maxwell's eq (5, 6) and the equations of motion of the electron (7) with the following result:

$$P = \frac{-\left[a_L \zeta + \frac{h_T h_L}{s(s^2 - h^2)} \right] \left[1 - a_L^2 - \zeta^2 - \frac{s}{s^2 - h^2} \right] + \left[a_L a_T - i \frac{h_L}{s^2 - h^2} \right] \left[a_T \zeta - i \frac{h_T}{s^2 - h^2} \right]}{\left[1 - a^2 - \frac{s^2 - h_L^2}{s(s^2 - h^2)} \right] \left[1 - a_L^2 - \zeta^2 - \frac{s}{s^2 - h^2} \right] - \left[a_T \zeta + i \frac{h_T}{s^2 - h^2} \right] \left[a_T \zeta - i \frac{h_T}{s^2 - h^2} \right]}, \quad (34)$$

$$Q = \frac{-\left[1 - a^2 - \frac{s^2 - h_L^2}{s(s^2 - h^2)} \right] \left[a_L a_T - i \frac{h_L}{s^2 - h^2} \right] + \left[a_T \zeta + i \frac{h_T}{s^2 - h^2} \right] \left[a_L \zeta + \frac{h_L h_T}{s(s^2 - h^2)} \right]}{\left[1 - a^2 - \frac{s^2 - h_L^2}{s(s^2 - h^2)} \right] \left[1 - a_L^2 - \zeta^2 - \frac{s}{s^2 - h^2} \right] - \left[a_T \zeta + i \frac{h_T}{s^2 - h^2} \right] \left[a_T \zeta - i \frac{h_T}{s^2 - h^2} \right]}, \quad (35)$$

where the particular slab, figure 2, $n=1, 2, 3 \dots p-1, p$, under consideration is designated by the notation, $\zeta = \zeta^{(n)}$, $P = P^{(n)}$, $Q = Q^{(n)}$, and, io, ie, ro, re refer to the four roots of the quartic in ζ for upgoing, downgoing, ordinary, and extraordinary waves respectively in the particular part z_n of the electron-ion plasma under consideration.

The ratio of the fields $Q = E_x/E_y$ and $P = E_z/E_y$ was introduced in the boundary conditions, eqs (24 to 28) as each slab was matched electrically to its adjacent slab such that the tangential \vec{E} and \vec{H} fields and the normal \vec{H} fields were continuous across the boundary. Notice that only the first four sets of boundary conditions, eqs (24 to 27), were employed in the matrix, eqs (33 to 34); the fifth boundary condition served as a check on the entire computation, since it is automatically satisfied by the other four conditions.

4. Monoenergetic Electron Collision Frequencies

The recent work of Jancel and Kahan [1955], Dingle, Arndt, and Roy [1956], Molmud [1958], and Phelps [1960] has treated the collision process in an electron-ion plasma with greater rigor. It can be shown, as a result of these investigations, that the average collision frequency, $g = \nu$, in the equation of motion of an electron (7) is an effective value independent of the energy, $u = kT/e$, where k is Boltzmann's constant, T is the temperature, degrees Kelvin. However, the investigations of Phelps [1960] indicate a strong dependence of the collision frequency upon the energy, u .

Phelps has developed integrals of the electron velocity or conductivity tensor. The integration over a Maxwellian energy distribution, $f_0 = [e/\pi kT]^{3/2} \exp[-eu/kT]$, involving a momentum transfer collision with gas molecules proportional to the energy u , $\nu = \nu(u)$ is accomplished for an electromagnetic wave of angular frequency, $\omega = 2\pi f$. The magnetic field is assumed to be vertical. The results of Phelps are generalized in this paper to a magnetic field of arbitrary direction and introduced into the analysis of the plasma model with a transitional electron-ion density described in this paper.

Indeed, Molmud [1959], demonstrated that the monoenergetic electron collision-frequency concept can be introduced into the equation of motion of the electron,

$$m \frac{d\bar{V}}{dt} + mg\bar{V} + \mu_0 e (\bar{V} \times \bar{H}_m) + e\bar{E} = 0, \quad (36)$$

as a new collision parameter, g , which has replaced the classical, ν . Thus, the classical theory implies, $g \sim \nu$.

The velocity, \bar{V} , tensor can be written,

$$\mathbf{J} = -NeV = \begin{bmatrix} A_1 A_2 A_3 \\ B_1 B_2 B_3 \\ C_1 C_2 C_3 \end{bmatrix} \begin{bmatrix} E_x \\ E_y \\ E_z \end{bmatrix}, \quad (37)$$

where

$$\begin{aligned} A_1 &= \frac{s(i\omega\epsilon_0)}{s^2 - h^2}, & B_1 &= \frac{-ih_L(i\omega\epsilon_0)}{s^2 - h^2}, & C_1 &= \frac{ih_T(i\omega\epsilon_0)}{s^2 - h^2}, \\ A_2 &= \frac{ih_L(i\omega\epsilon_0)}{s^2 - h^2}, & B_2 &= \frac{-(h_T^2 - s^2)(i\omega\epsilon_0)}{s(s^2 - h^2)}, & C_2 &= \frac{-h_L h_T(i\omega\epsilon_0)}{s(s^2 - h^2)}, \\ A_3 &= \frac{-ih_T(i\omega\epsilon_0)}{s^2 - h^2}, & B_3 &= \frac{-h_L h_T(i\omega\epsilon_0)}{s(s^2 - h^2)}, & C_3 &= \frac{(s^2 - h_L^2)(i\omega\epsilon_0)}{s(s^2 - h^2)}. \end{aligned}$$

The coefficients of the tensor matrix can be reduced to the form

$$\begin{aligned} A_1 &= \left[\frac{\left(-\frac{1}{2}\right)}{g(\Omega_1) + i\Omega_1} + \frac{\left(-\frac{1}{2}\right)}{g(\Omega_2) + i\Omega_2} \right] (-\omega_N^2 \epsilon_0), \\ A_2 &= \left[\frac{\left(-\frac{i}{2} \sin I\right)}{g(\Omega_1) + i\Omega_1} + \frac{\left(\frac{i}{2} \sin I\right)}{g(\Omega_2) + i\Omega_2} \right] (-\omega_N^2 \epsilon_0), \\ A_3 &= \left[\frac{\left(-\frac{i}{2} \cos I\right)}{g(\Omega_1) + i\Omega_1} + \frac{\left(\frac{i}{2} \cos I\right)}{g(\Omega_2) + i\Omega_2} \right] (-\omega_N^2 \epsilon_0), \\ B_1 &= \left[\frac{\left(\frac{i}{2} \sin I\right)}{g(\Omega_1) + i\Omega_1} + \frac{\left(-\frac{i}{2} \sin I\right)}{g(\Omega_2) + i\Omega_2} \right] (-\omega_N^2 \epsilon_0), \\ B_2 &= \left[\frac{(-\cos^2 I)}{g(\Omega_0) + i\Omega_0} + \frac{(-\frac{1}{2} \sin^2 I)}{g(\Omega_1) + i\Omega_1} + \frac{(-\frac{1}{2} \sin^2 I)}{g(\Omega_2) + i\Omega_2} \right] (-\omega_N^2 \epsilon_0), \\ B_3 &= \left[\frac{(\sin I \cos I)}{g(\Omega_0) + i\Omega_0} + \frac{(-\frac{1}{2} \sin I \cos I)}{g(\Omega_1) + i\Omega_1} + \frac{(-\frac{1}{2} \sin I \cos I)}{g(\Omega_2) + i\Omega_2} \right] (-\omega_N^2 \epsilon_0), \\ C_1 &= \left[\frac{\left(\frac{i}{2} \cos I\right)}{g(\Omega_1) + i\Omega_1} + \frac{\left(-\frac{i}{2} \cos I\right)}{g(\Omega_2) + i\Omega_2} \right] (-\omega_N^2 \epsilon_0), \\ C_2 &= \left[\frac{(\sin I \cos I)}{g(\Omega_0) + i\Omega_0} + \frac{(-\frac{1}{2} \sin I \cos I)}{g(\Omega_1) + i\Omega_1} + \frac{(-\frac{1}{2} \sin I \cos I)}{g(\Omega_2) + i\Omega_2} \right] (-\omega_N^2 \epsilon_0), \\ C_3 &= \left[\frac{(-\sin^2 I)}{g(\Omega_0) + i\Omega_0} + \frac{(-\frac{1}{2} \cos^2 I)}{g(\Omega_1) + i\Omega_1} + \frac{(-\frac{1}{2} \cos^2 I)}{g(\Omega_2) + i\Omega_2} \right] (-\omega_N^2 \epsilon_0), \end{aligned}$$

where $B_1 = -A_2$, $C_1 = -A_3$, $C_2 = B_3$, and where $\Omega_0 = \omega$, $\Omega_1 = \omega + \omega_H$, $\Omega_2 = \omega - \omega_H$. A quantity, Γ , is found by integrating over the velocity distribution for monoenergetic electron-ion collisions, $\nu(u)$, at each frequency, $\Omega = \Omega_0, \Omega_1, \Omega_2$,

$$\Gamma = -\frac{4\pi}{3} \int_0^\infty \frac{u^{3/2}}{[\nu(u) + i\Omega]} \frac{\partial}{\partial u} \left[\frac{e}{\pi k T} \right]^{3/2} \exp[-eu/kT] du, \quad (38)$$

which can be written in terms of Dingle, Arndt, and Roy [1956] tabulated functions, $\xi_{5/2}(x)$, $\xi_{3/2}(x)$,

$$\Gamma = \frac{1}{\Omega} \left[\frac{5}{2} \left(\frac{1}{\Upsilon} \right) \xi_{5/2} \left(\frac{1}{\Upsilon} \right) - i \left(\frac{1}{\Upsilon^2} \right) \xi_{3/2} \left(\frac{1}{\Upsilon} \right) \right], \quad (39)$$

where $\Upsilon = \nu(u)/\Omega$, $u = kT/e$, and $\nu(u) = akT/e = au$. The complex collision parameter, g , for the equation of motion can then be evaluated

$$g = \Gamma^{-1} - i\Omega = \frac{Re\Gamma - i[Im\Gamma + \Omega|\Gamma|^2]}{|\Gamma|^2}. \quad (40)$$

The quantity, g , is thus complex and there are three values corresponding to frequencies $\Omega = \Omega_0, \Omega_1, \Omega_2$. Furthermore, the value of g is also frequency dependent. The implication of the classical magneto-ionic theory that such a quantity can be represented by a real effective value without a frequency dependence is therefore not in general a valid concept.

The complex collision frequency, g , can be introduced into the analysis by evaluating the coefficients of the quartic (8 to 13) as follows:

$$a_4 = -\omega^2 \epsilon_0^2 (C_3 + i\omega \epsilon_0), \quad (41)$$

$$a_3 = -2\omega^2 \epsilon_0^2 a_L B_3, \quad (42)$$

$$a_2 = \omega^2 \epsilon_0^2 [A_1 + B_2 + 2C_3 - a_L^2 (B_2 + C_3) - a_T^2 (A_1 + C_3)] + i\omega \epsilon_0 [-A_1 C_3 - B_2 C_3 - A_3^2 + B_3^2 + 2\omega^2 \epsilon_0^2 (1 - a^2)] \quad (43)$$

$$a_1 = -2i\omega \epsilon_0 a_L (A_2 A_3 + A_1 B_3) - 2\omega^2 \epsilon_0^2 a_L B_3 (a^2 - 1) \quad (44)$$

$$\begin{aligned} a_0 = & A_1 B_2 C_3 - 2A_2 A_3 B_3 + A_3^2 B_2 - A_1 B_3^2 + A_2^2 C_3 + i\omega \epsilon_0 (A_1 C_3 + B_2 C_3 + A_1 B_2 + A_2^2 + A_3^2 - B_3^2) \\ & + i\omega \epsilon_0 a_T^2 (-A_1 C_3 - A_1 B_2 - A_3^2 - A_2^2) + i\omega \epsilon_0 a_L^2 (-B_2 C_3 - A_1 B_2 + B_3^2 - A_2^2) + \omega^2 \epsilon_0^2 (-A_1 - B_2 - C_3) \\ & + \omega^2 \epsilon_0^2 a_T^2 (2A_1 + B_2 + C_3) + \omega^2 \epsilon_0^2 a_L^2 (A_1 + 2B_2 + C_3) + \omega^2 \epsilon_0^2 a_T^2 a_L^2 (-A_1 - B_2) \\ & + \omega^2 \epsilon_0^2 a_T^4 (-A_1) - \omega^2 \epsilon_0^2 a_L^4 B_2 - i\omega^3 \epsilon_0^3 (1 - a^2)^2. \end{aligned} \quad (45)$$

The functions $\zeta_p(x)$ ($p = \frac{5}{2}, \frac{3}{2}$) can be evaluated by an application of quadrature techniques to the integrals [Johler and Walters, 1960], or other methods described by Dingle, and Roy [1956],

$$\zeta_{\frac{5}{2}}(x) = \left(\frac{5}{2}! \right) \int_0^\infty \rho^{\frac{5}{2}} (x^2 + \rho^2)^{-1} \exp(-\rho) d\rho, \quad (46)$$

$$\zeta_{\frac{3}{2}}(x) = \left(\frac{3}{2}! \right) \int_0^\infty \rho^{\frac{3}{2}} (x^2 + \rho^2)^{-1} \exp(-\rho) d\rho. \quad (47)$$

The quantities P and Q are rewritten,⁷ with the aid of eq (37), by substituting for s in eq (34, 35) the corresponding values of g , Ω_0 , Ω_1 , Ω_2 ,

$$P = \frac{-\left[a_L \zeta + \frac{B_3}{i\omega \epsilon_0} \right] \left[1 - a_L^2 - \zeta^2 + \frac{A_1}{i\omega \epsilon_0} \right] + \left[a_L a_T + \frac{A_2}{i\omega \epsilon_0} \right] \left[a_T \zeta - \frac{A_3}{i\omega \epsilon_0} \right]}{\left[1 - a^2 + \frac{C_3}{i\omega \epsilon_0} \right] \left[1 - a_L^2 - \zeta^2 + \frac{A_1}{i\omega \epsilon_0} \right] - \left[a_T \zeta + \frac{A_3}{i\omega \epsilon_0} \right] \left[a_T \zeta - \frac{A_3}{i\omega \epsilon_0} \right]}, \quad (48)$$

$$Q = \frac{-\left[1 - a^2 + \frac{C_3}{i\omega \epsilon_0} \right] \left[a_L a_T + \frac{A_2}{i\omega \epsilon_0} \right] + \left[a_T \zeta + \frac{A_3}{i\omega \epsilon_0} \right] \left[a_L \zeta + \frac{B_3}{i\omega \epsilon_0} \right]}{\left[1 - a^2 + \frac{C_3}{i\omega \epsilon_0} \right] \left[1 - a_L^2 - \zeta^2 + \frac{A_1}{i\omega \epsilon_0} \right] - \left[a_T \zeta + \frac{A_3}{i\omega \epsilon_0} \right] \left[a_T \zeta - \frac{A_3}{i\omega \epsilon_0} \right]}. \quad (49)$$

⁷ The constant ϵ_0 or the factor $i\omega \epsilon_0$ can be eliminated from eq (37, 41-45, 48, and 49) for convenience. The factor was retained so that eq (37), would be correct dimensionally, i.e., J = current, amperes per square meter.

5. Computations and Discussion

The reflection coefficients, figures 5–24, were evaluated for the continuous electron-ion density transition, figures 3 and 4, with the aid of the classical magneto-ionic theory. The typical daytime-noon profile, figure 3 [Waynick, 1957], was selected to represent a quiescent ionosphere. The disturbed profile, figure 3 [Seddon and Jackson, 1958], was also selected to give an indication of the intensity of the ionization during disturbed conditions. The region of the ionosphere below 1,000 electrons/cm³ was represented with a Gaussian electron density-altitude distribution [Budden, 1955],

$$N = N_{\max} \exp [-(z - z_{\max})^2/k'],$$

where the constants N_{\max} , z_{\max} , and k' were determined by the measured profile, >1,000 electrons/cm³. In particular, $N_{\max} = 26,000$ electrons/cm³, $z_{\max} = 85,000$ m, $k' = 1.92 \times 10^8$. This profile was measured during a high-frequency ionosonde blackout observed at Ft. Churchill, Canada, 1332 CST, 15 November 1956. Data was therefore made available in the theoretical form of a continuous electron-ion density transition for a model plasma which represents approximate conditions of the ionosphere during disturbed phenomena. This ionosonde blackout is classified as a local auroral-zone blackout which is confined to the auroral zone or some segment thereof.

The Nicolet/3 collision frequency [Nicolet, 1958; Sedden and Jackson, 1958] was employed in this analysis. Other profiles, $\nu(h)$, are illustrated, figure 3 [Compton, et al., 1953; Gardner and Pawsey, 1953; Fejer, 1955]. These collision frequencies are applicable to the classical magneto-ionic theory employing the approximation, $g \sim \nu$ in the equation of motion (7) of the electron. Recently Kane [1959 and 1960] re-evaluated the profile, $\nu(h)$, on the basis of monoenergetic electron collisions, $\nu = \nu(u)$, from which the complex parameter, g , can be deduced. Furthermore, the reflection coefficients presented in this paper can be re-evaluated with the aid of such data and the theory of the monoenergetic electron collision frequency, which task will be reported separately for comparison with the classical theory.

The computation of the field strength of a radio wave propagated about the earth is dependent upon the reflection process at the ionosphere [Johler, 1961 b and c] and the mode theory [Wait, 1960] or a geometric-optical theory requires the introduction of reflection coefficients into the analysis. Thus, the essential nature of ionospheric propagation is described by the reflection coefficients, T_{ee} , T_{em} , for vertical polarization, and T_{mm} , T_{me} for horizontal.

The reflection coefficients, T_{ee} , T_{em} , T_{me} , T_{mm} , were evaluated, figures 5 through 11. For the typical daytime-noon model ionosphere as a function of frequency, $f = 10$ kc/s to 1,000 kc/s, with various values of magnetic azimuth, $\phi_a = 0, 45, 90, 135, 180, 225, 270, 315$ deg; at a temperate magnetic latitude, $I = 60$ deg, assuming a typical magnetic field intensity; $H_m = 0.5$ gauss and grazing incidence transmission, $\phi_i = 81.79$ deg ($d = 1,000$ statute miles for a single-hop geometric-optical transmission).

The reflection coefficients, $|T_{ee}|$, $|T_{mm}|$ show a steady decrease in amplitude as the frequency is increased. A small, perceptible rise is noted near the gyrofrequency, however. Such a steady decrement in amplitude could be imitated by the sharply bounded model ionosphere. [Johler, 1961 b and c] by suitable selection of a fictitious low-electron density. But such a model is a primitive theoretical representation of the true reflection process.

The magnitude of the abnormal components, $|T_{em}|$, $|T_{me}|$ also show a decrement as a function of frequency. But these components are quite small (< 0.1 at 10 kc/s, for example). The corresponding disturbed-blackout reflection coefficients are also illustrated. The angle of incidence, ϕ_i , was changed slightly as a result of a lowering of the ionosphere. The principal cause of change as a result of this profile is nevertheless the re-distribution of the $N(h)$ profile from the quiescent to the disturbed conditions. It is interesting to note an increased attenuation at the higher frequencies, 100 to 1,000 kc/s. However, the high attenuation or ionosonde blackout which characterizes high frequencies does not seem to exist. Indeed, an enhancement

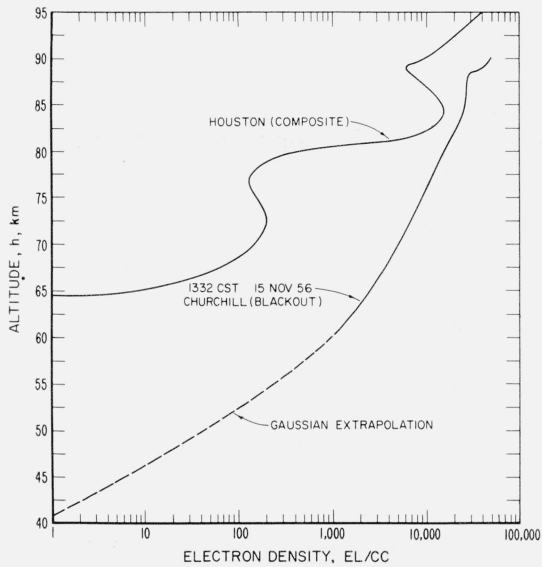


FIGURE 3. Electron density-altitude profiles $N(h)$ (quiescent and disturbed-blackout) employed in the analysis.

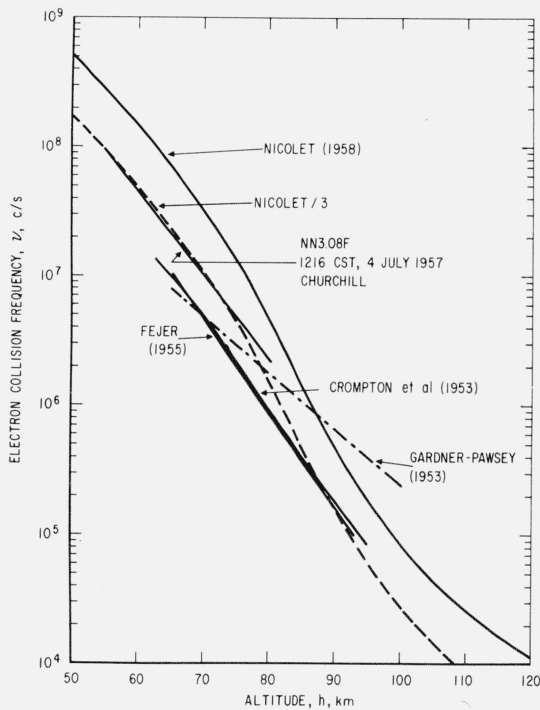


FIGURE 4. Collision frequency-altitude profiles $\nu(h)$ for classical magneto-ionic theory.

Nicolet/3 was employed in the analysis.

in the field is anticipated from this profile at VLF (<30 kc/s). Whereas there is no experimental evidence to establish the non-existence of ionosonde blackout phenomena at LF/VLF, a search of the literature did not reveal any report of very high attenuation of LF/VLF during such D -region events.

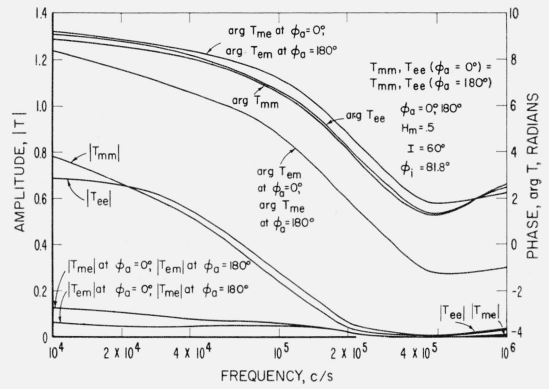


FIGURE 5. Reflection coefficients (amplitude and phase) of the lower ionosphere for low frequencies, illustrating the frequency dependence of the classical theory $\phi_a=0, 180$.

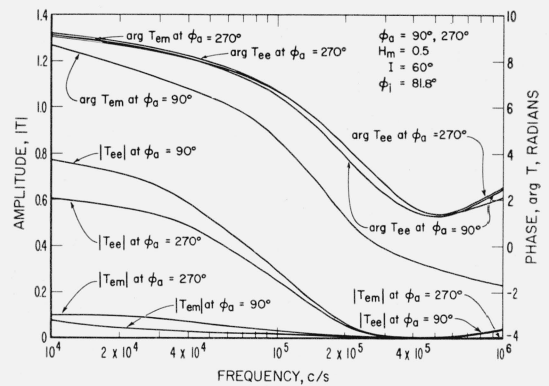


FIGURE 6. Reflection coefficients (amplitude and phase) of the lower ionosphere for low frequencies illustrating the frequency dependence of the classical theory, $\phi_a=90, 270$, vertical polarization, T_{ee}, T_{em} .

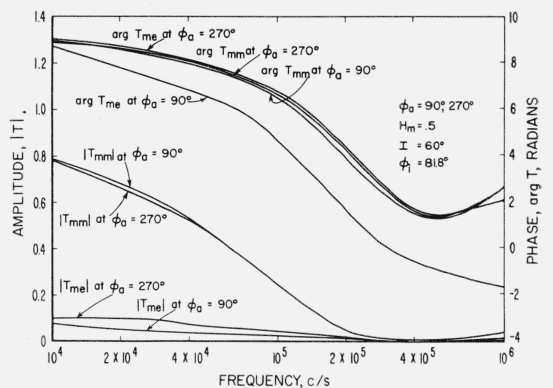


FIGURE 7. Reflection coefficients (amplitude and phase) of the lower ionosphere for low frequencies illustrating the frequency dependence of the classical theory, $\phi_a=90, 270$, horizontal polarization, T_{mm}, T_{me} .

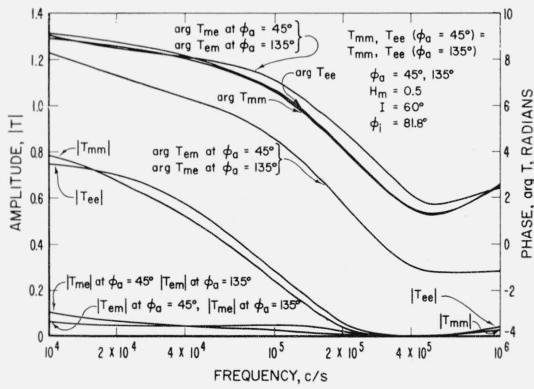


FIGURE 8. Reflection coefficients (amplitude and phase) of the lower ionosphere for low frequencies illustrating the frequency dependence of the classical theory, $\phi_a = 45, 135$.

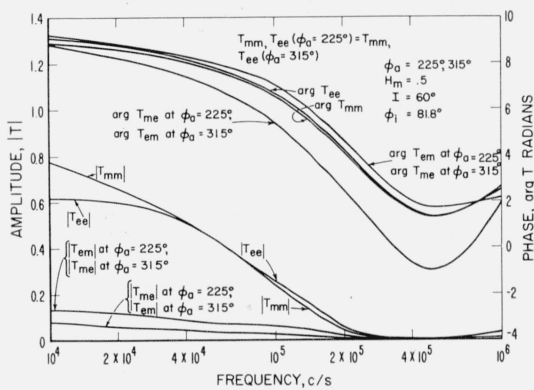


FIGURE 9. Reflection coefficients (amplitude and phase) of the lower ionosphere for low frequencies illustrating the frequency dependence of the classical theory, $\phi_a = 225, 315$.

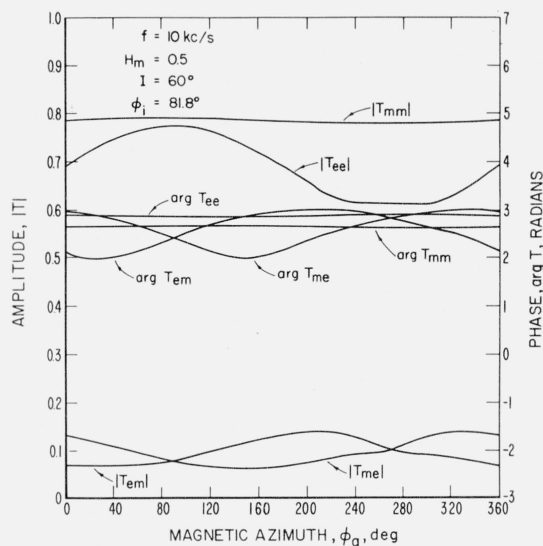


FIGURE 10. Reflection coefficients (amplitude and phase) of the lower ionosphere for low frequencies illustrating the action of the Lorentzian force (earth's magnetic field) $f = 10$ kc/s.

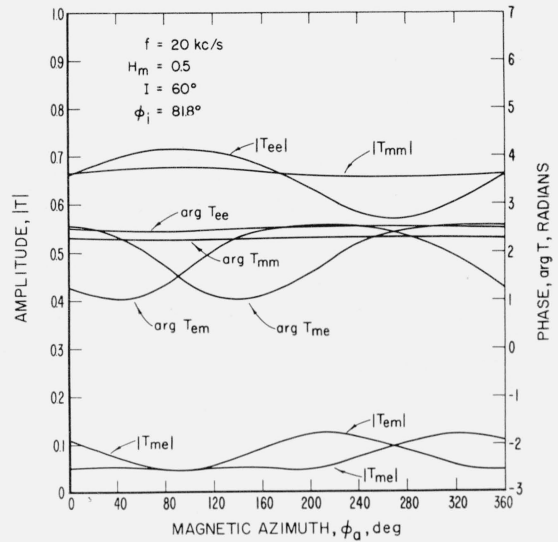


FIGURE 11. Reflection coefficients (amplitude and phase) of the lower ionosphere for low frequencies illustrating the action of the Lorentzian force (earth's magnetic field) in the classical theory, $f = 20$ kc/s.

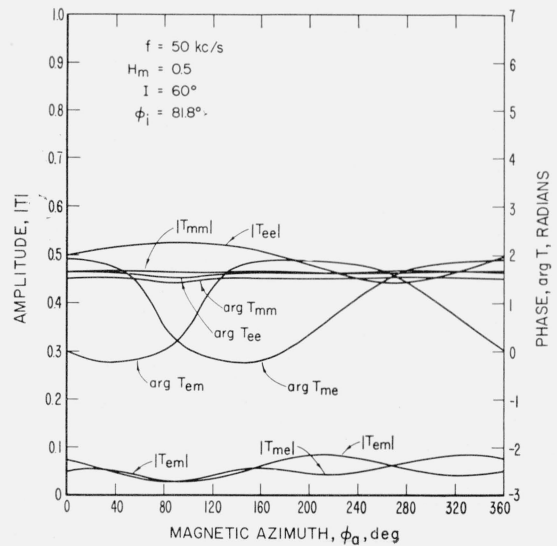


FIGURE 12. Reflection coefficients (amplitude and phase) of the lower ionosphere for low frequencies illustrating the action of the Lorentzian force (earth's magnetic field) in the classical theory, $f = 50$ kc/s.

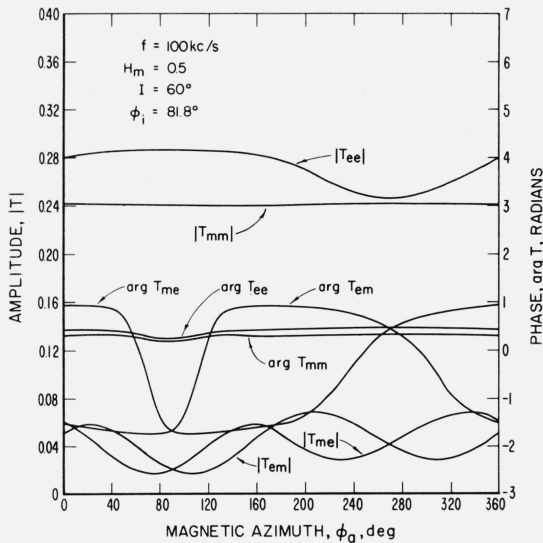


FIGURE 13. Reflection coefficients (amplitude and phase) of the lower ionosphere for low frequencies illustrating the action of the Lorentzian force (earth's magnetic field) in the classical theory, $f=100$ kc/s.

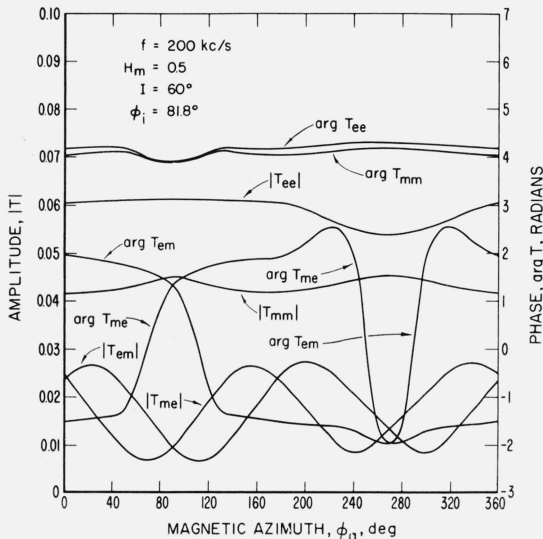


FIGURE 14. Reflection coefficients (amplitude and phase) of the lower ionosphere for low frequencies illustrating the action of the Lorentzian force (earth's magnetic field) in the classical theory, $f=200$ kc/s.

The effect of the Lorentz force, $\mu_0 e(\vec{V} \times \vec{H}_m)$, (7) or the action of the earth's magnetic field, on the reflection process is also illustrated, figures 12 through 15. The reflection coefficients are illustrated as a function of the magnetic azimuth, ϕ_a . It is interesting to note that, as in the case of the sharply bounded model [Johler, 1961a], the propagation into the west, $\phi_a=270^\circ$, shows a smaller reflection coefficient than the propagation into the east, $\phi_a=90^\circ$. Thus, there is clearly a non-reciprocity (interchange of transmitter and receiver) in the propagation which enhances the field propagated into the east relative to the field propagated into the west. However, the characteristic variation with respect to magnetic azimuth is considerably masked at the higher frequencies (>200 kc/s) for the highly absorbing daytime-noon model ionosphere employed.

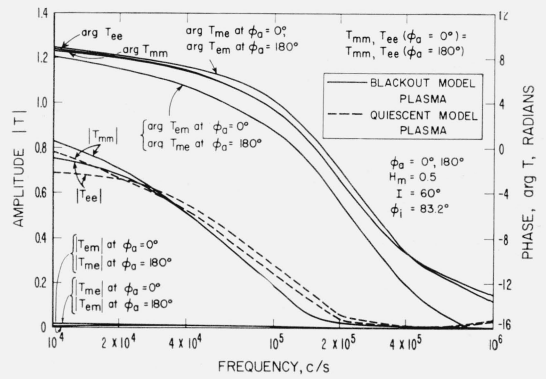


FIGURE 15. Reflection coefficients (amplitude and phase) of the lower ionosphere for low frequencies during blackout conditions illustrating the frequency dependence of the classical magneto-ionic theory.

$|T_{ee}|$ and $|T_{mm}|$ are also illustrated for comparison with quiescent conditions (see fig. 5-9 for complete quiescent reflection coefficients). $\phi_a=0, 180$.

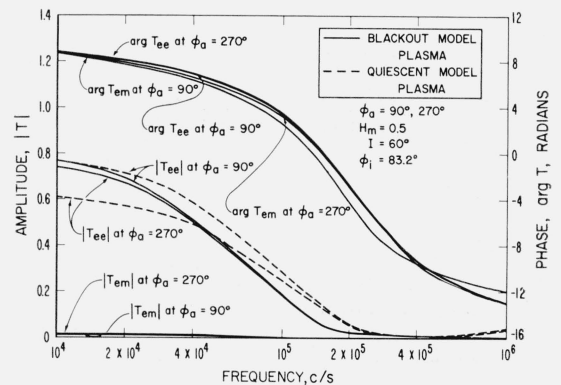


FIGURE 16. Reflection coefficients (amplitude and phase) of the lower ionosphere for low frequencies during blackout conditions illustrating the frequency dependence of the classical magneto-ionic theory.

$|T_{ee}|$ and $|T_{mm}|$ are also illustrated for comparison with quiescent conditions (see fig. 5-9 for complete quiescent reflection coefficients). $\phi_a=90, 270$, vertical polarization, T_{ee}, T_{em} .

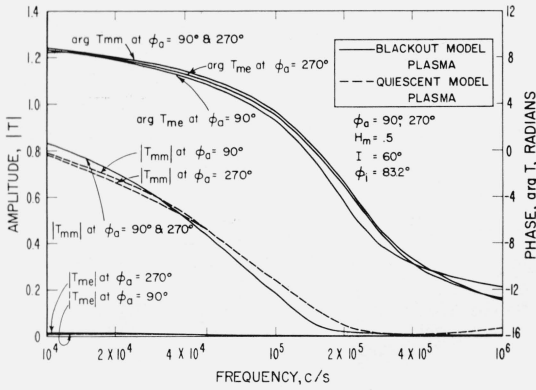


FIGURE 17. Reflection coefficients (amplitude and phase) of the lower ionosphere for low frequencies during blackout conditions illustrating the frequency dependence of the classical magneto-ionic theory.

$|T_{ee}|$ and $|T_{mm}|$ are also illustrated for comparison with quiescent conditions (see fig. 5-9 for complete quiescent reflection coefficients). $\phi_0=90, 270$, horizontal polarization, T_{mm}, T_{me} .

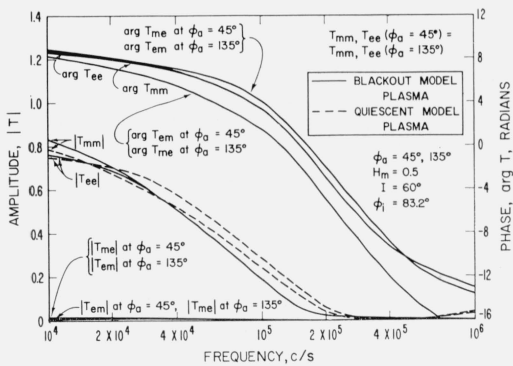


FIGURE 18. Reflection coefficients (amplitude and phase) of the lower ionosphere for low frequencies during blackout conditions illustrating the frequency dependence of the classical magneto-ionic theory.

$|T_{ee}|$ and $|T_{mm}|$ are also illustrated for comparison with quiescent conditions (see fig. 5-9 for complete quiescent reflection coefficients). $\phi_0=45, 135$.

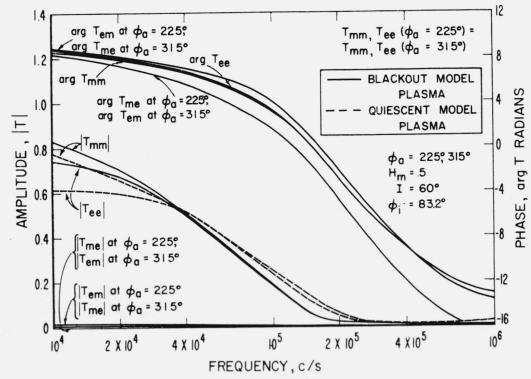


FIGURE 19. Reflection coefficients (amplitude and phase) of the lower ionosphere for low frequencies during blackout conditions illustrating the frequency dependence of the classical magneto-ionic theory.

$|T_{ee}|$ and $|T_{mm}|$ are also illustrated for comparison with quiescent conditions (see fig. 5-9 for complete quiescent reflection coefficients). $\phi_0=225, 315$.

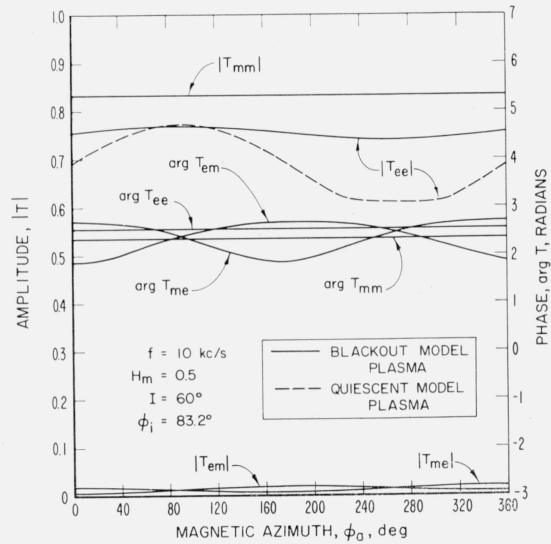


FIGURE 20. Reflection coefficients (amplitude and phase) of the lower ionosphere for low frequencies illustrating the action of the Lorentzian force (earth's magnetic field) in the classical magneto-ionic theory during blackout conditions.

$|T_{ee}|$ also shown for comparison with quiescent conditions. (See fig. 10-14 for complete quiescent reflection coefficients.) $f=10$ kc/s.

6. Conclusions

The reflection coefficients of the lower ionosphere can be more rigorously determined from geophysical data on the lower ionosphere with the aid of techniques developed in this paper. The classical magneto-ionic theory can be employed, but is subject to restrictions as to the use of the average collision frequency, $g \sim \nu$. It is therefore concluded that the same problem should be re-investigated with the aid of the monoenergetic electron collision frequency and the formulation presented in this paper for the determination of the complex parameter, g ; comparison can then be made with the classical theory.

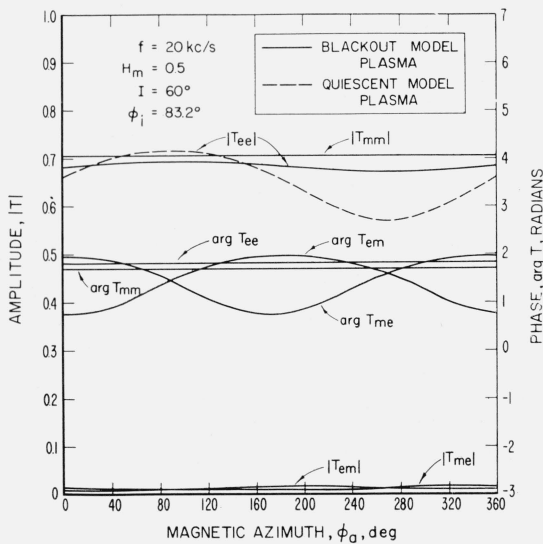


FIGURE 21. Reflection coefficients (amplitude and phase) of the lower ionosphere for low frequencies illustrating the action of the Lorentzian force (earth's magnetic field) in the classical magneto-ionic theory during blackout conditions.

$|T_{ee}|$ also shown for comparison with quiescent conditions. (See fig. 10-14 for complete quiescent reflection coefficients.) $f=20$ kc/s.

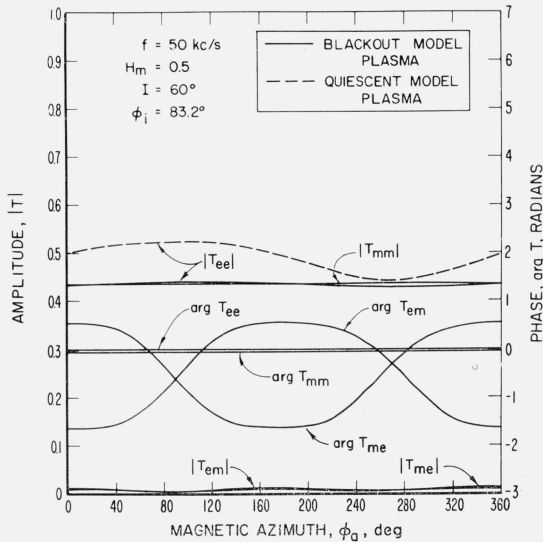


FIGURE 22. Reflection coefficients (amplitude and phase) of the lower ionosphere for low frequencies illustrating the action of the Lorentzian force (earth's magnetic field) in the classical magneto-ionic theory during blackout conditions.

$|T_{ee}|$ also shown for comparison with quiescent conditions. (See fig. 10-14 for complete quiescent reflection coefficients.) $f=50$ kc/s.

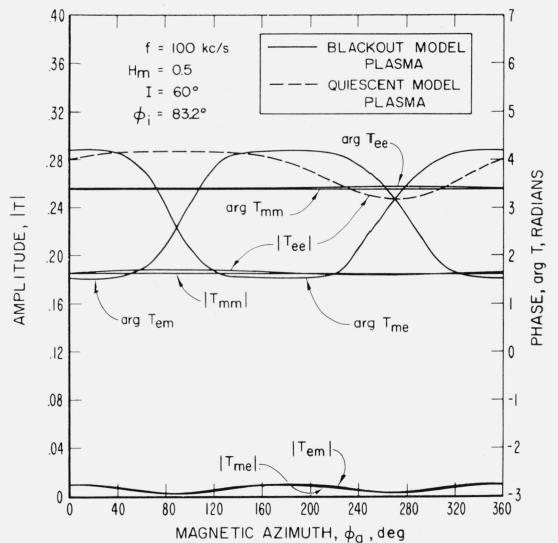


FIGURE 23. Reflection coefficients (amplitude and phase) of the lower ionosphere for low frequencies illustrating the action of the Lorentzian force (earth's magnetic field) in the classical magneto-ionic theory during blackout conditions.

$|T_{ee}|$ also shown for comparison with quiescent conditions. (See fig. 10-14 for complete quiescent reflection coefficients.) $f=100$ kc/s.

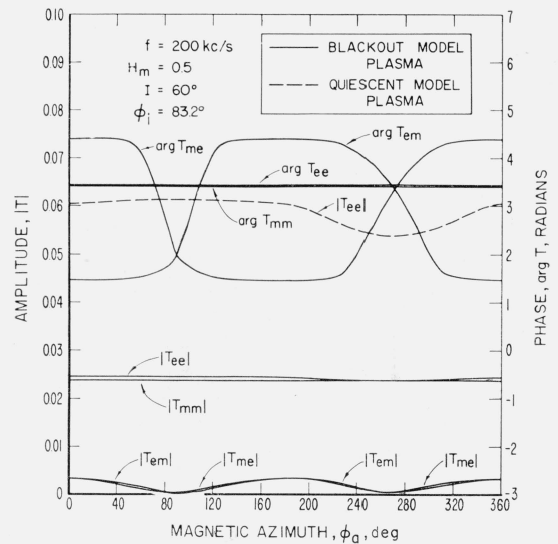


FIGURE 24. Reflection coefficients (amplitude and phase) of the lower ionosphere for low frequencies illustrating the action of the Lorentzian force (earth's magnetic field) in the classical magneto-ionic theory during blackout conditions.

$|T_{ee}|$ also shown for comparison with quiescent conditions. (See fig. 10-14 for complete quiescent reflection coefficients.) $f=200$ kc/s.

The results of this investigation indicate that the total blackout phenomena which characterize HF do not extend through LF and VLF for the model ionosphere investigated with the classical theory. Indeed, for the situations computed here the field was found to be enhanced at VLF. The employment of these models does not alter previous conclusions on the action of the Lorentz force on the electron in the ionosphere, i.e., the propagation into the east is enhanced with respect to the propagation into the west, except to a lesser degree at the higher frequencies, which also exhibit increased attenuation.

7. References

- Booker, H. G., Some general properties of the formulae of the magneto-ionic theory, *Proc. Roy. Soc. (London)* **A147**, 352–382 (Nov. 1934).
- Brekhovskikh, L. M., *Waves in layered media* (Academic Press, Inc., New York, N.Y., 1960).
- Budden, K. G., The numerical solution of the differential equations governing the reflection of long radio waves from the ionosphere II, *Phil. Trans. Roy. Soc. London*, **A248**, 45–72 (1955).
- Compton, R. W., L. G. H. Huxley, and D. J. Sutton, Experimental studies of the motions of slow electrons in air with applications to the ionosphere, *Proc. Roy. Soc. (London)* **A218**, 507–519 (July 1953).
- Dingle, R. B., D. Arndt, and S. K. Roy, The integrals $\xi_p(x)$ and $D_p(x)$ and their tabulation, *Appl. Sci. Research* **6B**, 155–164 (1956).
- Fejer, J. A., The interaction of pulsed radio waves in the ionosphere, *J. Atmospheric and Terrest. Phys.* **7**, 322–332 (Dec. 1955).
- Ferraro, A. J., and J. J. Gibbons, Polarization computations by means of multislabs approximation, *J. Atmospheric and Terrest. Phys.* **16**, 131 (1959).
- Gardner, F. F., and J. L. Pawsey, Study of the ionospheric D-region using partial reflections, *J. Atmospheric and Terrest. Physics* **3**, 321–344 (July 1953).
- Hines, C. O., Wave packets, the Poynting vector and energy flow, pts. I–IV, *J. Geophys. Research* **56** (Mar., June–Dec. 1951).
- Jancel, R., et T. Kahan, Théorie du couplage des ondes électromagnétiques ordinaire et extraordinaire dans un plasma inhomogène et anisotrope et conditions de réflexion, *J. Physique et Radian* **15**, 136–145 (1955).
- Johler, J. R., Magneto-ionic propagation phenomena in low- and very low-radiofrequency waves reflected by the ionosphere, *J. Research NBS* **65D** (Radio Prop.) No. 1, 53–65 (Jan.–Feb. 1961a).
- Johler, J. R., On LF ionospheric phenomena in radio navigation systems, Avionics Panel Meeting of the Advisory Group for Aeronautical Research and Development (AGARD), 3–8 October 1960, Istanbul, Turkey, of Organisation du Traité de l'Atlantique Nord, 64, rue de Varenne, Paris 7ème (to be published, Pergamon Press, 1961b).
- Johler, J. R., On the analysis of LF ionospheric phenomena, *J. Research NBS* **65D** (Radio Prop.) No. 5, 507 (Sept.–Oct. 1961c).
- Johler, J. R., and L. C. Walters, On the theory of reflection of low- and very low-radiofrequency waves from the ionosphere, *J. Research NBS* **64D** (Radio Prop.) No. 3, 239–285 (May–June 1960).
- Kane, J. A., Arctic measurements of electron collision frequencies in the D-region of the ionosphere, *J. Geophys. Research* **64**, No. 2, 133–139 (Feb. 1959).
- Kane, J. A., Re-evaluation of ionospheric electron densities and collision frequencies derived from rocket measurements of refractive index and attenuation, IGY Rocket Report No. 6, p. 135, National Acad. Sci., Washington, D. C. (Nov. 1960).
- Molmud, P., Langevin equation and the ac conductivity of non-maxwellian plasmas, *J. Phys. Res.* **114**, No. 1, 29–32 (Apr. 1959).
- Nicolet, M., Aeronomic conditions in the mesosphere and lower ionosphere, Science Report No. 102, Pennsylvania State Univ., Univ. Park, Pennsylvania (Apr. 1958).
- Phelps, A. V., Propagation constants for electromagnetic waves in weakly ionized, dry air, *J. of Applied Physics* **21**, No. 10, 1723–1729 (Oct. 1960).
- Seddon, J. C., and J. E. Jackson, Rocket Arctic ionosphere measurements, IGY Rocket Report Series, No. 1, 140–148 (July 1958).
- Wait, J. R., Terrestrial propagation of VLF radio waves, *J. Research NBS* **64D** (Radio Prop.) No. 2 (Mar.–Apr. 1960).
- Wait, J. R., Some boundary value problems involving plasma media, *J. Research NBS* **65B** (Math. and Math. Phys.), No. 2, 137–150 (Apr.–June 1961).
- Waynick, A. H., The present state of knowledge concerning the lower ionosphere, *Proc. IRE* **45**, No. 6, 741–749 (June 1957).